american physiological society

JNP JOURNAL OF NEUROPHYSIOLOGY

J Neurophysiol 127: 1363–1387, 2022.
First published April 13, 2022; doi:10.1152/jn.00279.2021

RESEARCH ARTICLE

Control of Movement

Functional characterization of the fronto-parietal reaching and grasping network: reversible deactivation of M1 and areas 2, 5, and 7b in awake behaving monkeys

Adam B. Goldring,[1,2] Dylan F. Cooke,[2,3] Carlos R. Pineda,[1,2] Gregg H. Recanzone,[2,4] and Leah A. Krubitzer[1,2]

[1]*Department of Psychology, University of California, Davis, California;* [2]*Center for Neuroscience, University of California, Davis, California;* [3]*Department of Biomedical Physiology and Kinesiology (BPK), Simon Fraser University, Burnaby, British Columbia, Canada; and* [4]*Department of Neurobiology, Physiology and Behavior, University of California, Davis, California*

Abstract

In the present investigation, we examined the role of different cortical fields in the fronto-parietal reaching and grasping network in awake, behaving macaque monkeys. This network is greatly expanded in primates compared to other mammals and coevolved with glabrous hands with opposable thumbs and the extraordinary dexterous behaviors employed by a number of primates, including humans. To examine this, we reversibly deactivated the primary motor area (M1), anterior parietal area 2, and posterior parietal areas 5L and 7b individually while monkeys were performing two types of reaching and grasping tasks. Reversible deactivation was accomplished with small microfluidic thermal regulators abutting specifically targeted cortical areas. Placement of these devices in the different cortical fields was confirmed post hoc in histologically processed tissue. Our results indicate that the different areas examined form a complex network of motor control that is overlapping. However, several consistent themes emerged that suggest the independent roles that motor cortex, area 2, area 7b, and area 5L play in the motor planning and execution of reaching and grasping movements. Area 5L is involved in the early stages and area 7b the later stages of a reaching and grasping movement, motor cortex is involved in all aspects of the execution of the movement, and area 2 provides proprioceptive feedback throughout the movement. We discuss our results in the context of previous studies that explored the fronto-parietal network, the overlapping (but also independent) functions of different nodes of this network, and the rapid compensatory plasticity of this network.

NEW & NOTEWORTHY This is the first study to directly compare the results of cooling different portions of the fronto-parietal reaching and grasping network (motor cortex, anterior and posterior parietal cortex) in the same animals and the first to employ a complex, bimanual reaching and grasping task that is ethologically relevant. Whereas cooling area 7b or area 5L evoked deficits at distinct task phases, cooling M1 evoked a general set of deficits and cooling area 2 evoked proprioceptive deficits.

area 2; area 5; area 7b; cortical deactivation; reaching

INTRODUCTION

The extraordinary degree to which humans can interact with and change the world around them can be attributed, in large part, to the evolution of the hands and the complex, dexterous ways in which they are used. Our remarkable manual abilities emerged with the coevolution of the hand and motor and posterior parietal cortical areas that program and control manual prehension. The posterior parietal cortex (PPC) comprises a constellation of areas that differ in their function as well as in the effectors that they help control (see Fig. 1) (see Table 1 for abbreviations/structures). However, a common feature of these areas is that they sit at the interface of perception and action, combining the sensory information from several modalities with effector kinematics to compute various movements tailored to specific

Correspondence: L. A. Krubitzer (lakrubitzer@ucdavis.edu).
Submitted 22 June 2021 / Revised 4 April 2022 / Accepted 4 April 2022

Table 1. *Abbreviations*

Body parts	
D1–5	Digits 1–5
Cortical fields and structures	
1	Area 1; cutaneous representation caudal to area 3b
2	Area 2; representation of deep receptors caudal to area 1
3b	Area 3b, primary somatosensory area, S1 proper
5L	Area 5, lateral division [as defined in Seelke et al. (7)]
5M	Area 5, medial division
7b	Area 7b; posterior parietal area on the inferior parietal lobule
AIP	Anterior intraparietal area
ARC	Arcuate sulcus
CS	Central sulcus
IPS	Intraparietal sulcus
LIP	Lateral intraparietal area
LS	Lateral sulcus
LUN	Lunate sulcus
M1	Primary motor cortex
MIP	Medial intraparietal area
PE	Superior parietal lobe area
PEc	Superior parietal lobe area (caudal portion)
PF	Parietal area F; overlaps 7b
PFG	Parietal area FG; overlaps 7b
PG	Parietal area G
PM(d, v)	Premotor cortex (dorsal or ventral division)
PCD	Postcentral dimple
PS	Principal sulcus
STS	Superior temporal sulcus
VIP	Ventral intraparietal area

objects and contexts (see Refs. 1, 2 for review). Furthermore, although many of these regions seem specialized for specific actions using specific body parts, overlapping effector and movement representations as well as a mixed selectivity schema highlight the importance of considering these regions as part of a dynamic, robust network that controls ethologically critical actions in primates (see Ref. 3 for review). Recent cluster-based metanalyses of intrinsic and extrinsic connections of these areas suggest that they may be grouped into functional domains. Several of these parietal domains, together with frontal motor, cingulate, and prefrontal cortical domains, form at least two parallel systems within the fronto-parietal reaching and grasping network that allow primates to so successfully interact with and manipulate their environment (4).

In rhesus macaques it is generally agreed that Brodmann's areas 5 and 7 compose a significant proportion of the PPC (see Refs. 5, 6 for review). These two, large, architectonically defined regions of cortex have been subsequently subdivided into multiple cortical fields based on both functional and anatomical criteria (Fig. 1). For example, modern anatomical techniques have parcellated area 5 into several overlapping subfields with differing nomenclature (13–15). Because of the variability of recording locations within this relatively large area and the diversity of behavioral tasks employed to study it (see Ref. 7 for review), this region has been implicated in such diverse processes as coding of reach intention (16–18), reach and grasp kinematics (19, 20), online monitoring of different reach styles during object approach (21–23), and the coordinate transformation of reach targets into body- and shoulder-centered coordinates (24, 25) or eye-centered reference frames (26). Recent efforts by our laboratory have characterized one such subfield, area 5L, which has a distinct electrophysiological, architectonic (7), and connectional (27) profile, distinguishing it from adjacent fields area 2 and VIP.

Much like area 5, anatomical investigations have divided Brodmann's area 7 into overlapping regions with various nomenclatures (13–15, 28–31). Neurons in area 7a are primarily responsive to visual stimuli, eye movements, and arm movements related to reaching and grasping. Area 7b neurons are primarily responsive to somatosensory stimulation of the arm, hand, and mouth; those that respond during movement are predominantly related to hand use, orofacial movements, and hand-mouth coordination (8, 32–34).

Although a number of cortical areas that compose PPC have been the subject of extensive electrophysiological investigations, manipulation-of-function studies are limited. Lesions to various portions of area 5 and area 7 produce profound deficits. However, those deficits are often fleeting unless a substantially large portion of cortex is removed (35–39). Furthermore, the rapid recovery associated with lesions to these areas is likely accompanied by compensatory reorganization of spared regions, making interpretation of these results difficult. Chemical inactivation with agents such as muscimol have provided insight into the function of regions such as PE/PEc (40, 41), parietal reach region (PRR) (42–47), caudal intraparietal area (CIP) (48), and LIP (48–52), but these methods present their own difficulties, such as slow onset and recovery time as well as potentially imprecise spread of the chemical agent outside of the region of interest unless accompanied by simultaneous recording or imaging (see Refs. 53, 54 for review). Improvements in optogenetic methods in nonhuman primates show promise for investigating these regions, but these techniques have so far only been used to investigate relatively small, well-studied portions of the PPC (55).

Over the past several decades, transient cooling has emerged as a relatively simple but effective method for quickly and reversibly disrupting the function of a variety of cortical regions (54, 56). In awake, behaving macaques cooling has been used extensively to study the visual system (e.g., Refs. 57–60), prefrontal cortex (e.g., Refs. 61–64), and the role of LIP in driving visual salience signals in prefrontal cortex and subsequently selecting saccade targets (65). To our knowledge, however, studies that have examined the effect of cooling PPC in awake, behaving animals executing skilled limb movements have been limited to large deactivations of multiple subregions of area 5 or area 7 (66, 67) or, more recently, cooling a portion of area 5 on the gyral surface while monkeys perform a reaching perturbation task (68). Whereas the former study did not examine the contribution of individual subregions, the latter study examined reaching in a nonethological context that did not include any grasping behaviors. Furthermore, to our knowledge no studies have examined the effects of cooling area 7b on reaching and grasping behavior and hand to mouth feeding.

We have recently investigated the influence of cooling different areas of the PPC in anesthetized macaques to probe the role of feedforward and feedback interactions within the fronto-parietal reaching and grasping network (69, 70). We found that cooling either of the two regions within PPC (area 5L or area 7b) induced rapid changes in the size and shape of

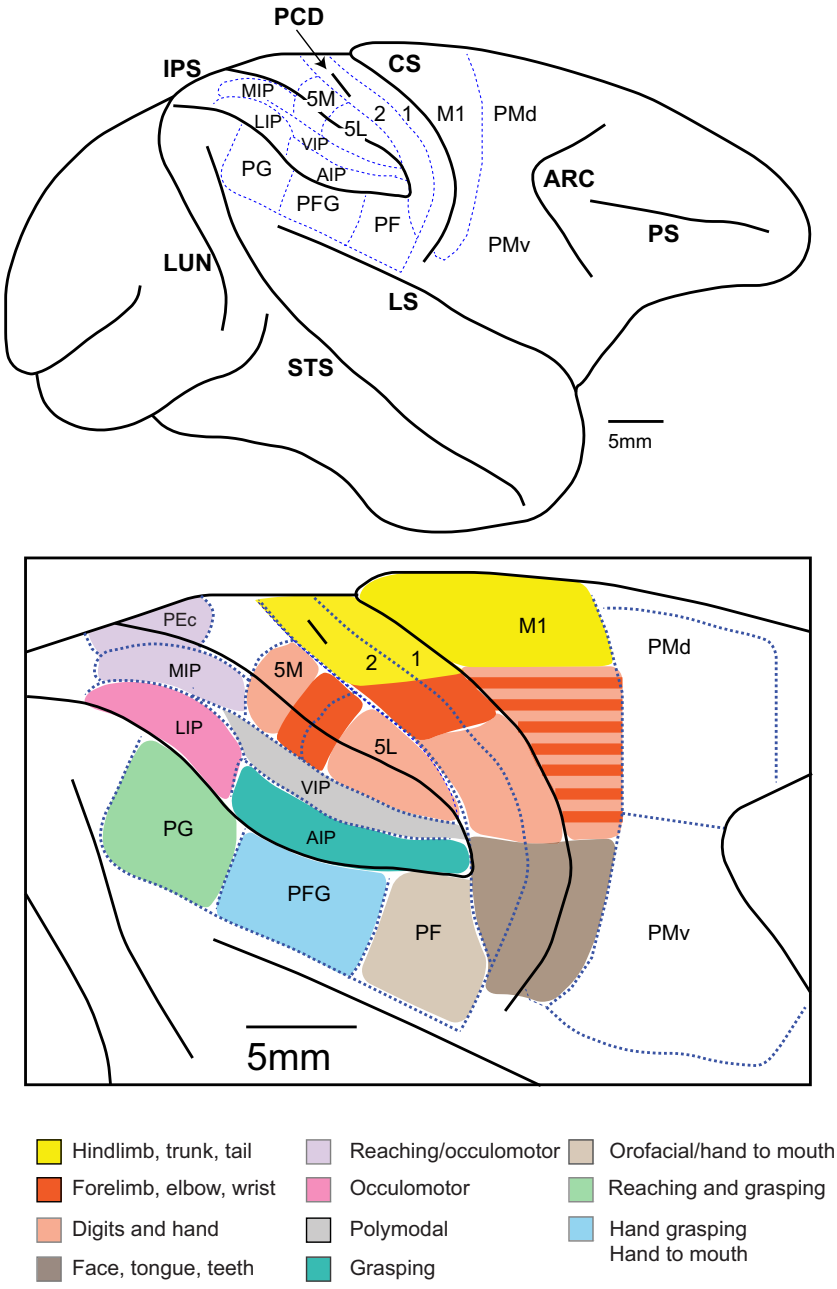

Figure 1. *Top*: the location of cortical fields associated with the reaching and grasping network in macaque monkeys relative to major sulci. *Bottom*: the topographic organization of motor and somatosensory cortex and the rough topographic organization of areas 5M and 5L. The functional organization of areas in and around the IPS is derived from a number of studies including Refs. 4, 7–12. It should be noted that the nomenclature, function, and relative location of areas in the IPS often differ between laboratories (see Table 1 for abbreviations).

receptive fields of neurons located in anterior parietal cortex (areas 1 and 2), whereas cooling M1 had little to no effect on areas 1 and 2. Given the location of these somatosensory receptive fields (hand and forelimb), these studies suggest that anterior and posterior parietal cortex form part of a reciprocally connected network associated with manual behavior.

Here we examine the effects of reversibly deactivating four different cortical areas (motor cortex, area 2, area 7b, and area 5L) in the fronto-parietal reaching and grasping network while monkeys performed two different manual tasks. One task required an accurate reach trajectory to retrieve a food reward with one hand but permitted the use of a variety of grasp types to do so. The three distinct phases of this task (early reaching, middle grasping, and late feeding) allowed us to assess the hypothesized role that several of our regions of interest play in manual behavior (see *Behavioral Tasks*).

The other, more difficult task required both bimanual coordination and the use of a D1-D2 (thumb and forefinger) precision grip to retrieve a food reward. Although similar to the reach task in that it contains both an initial reach into the task workspace and an end stage involving feeding, the most difficult portion of this task involves manipulating a weighted cylinder with one hand to expose a food pellet located in a small well that can only be retrieved by using some sort of precision grip executed with the other hand (see *Behavioral Tasks*).

Both tasks were executed with and without visual feedback to determine whether any evoked deficits were

driven by errors of somatosensation/proprioception and whether visualizing the target/effector changed performance in a way that suggested errors of multisensory integration or reference frame transformation. We found that cooling different regions produced overlapping but distinct deficits largely consistent with their hypothesized roles. Although these roles are based on previous ablation and correlative electrophysiological studies; our data provide uniquely precise causal data free from postinjury plasticity. Taken together, these results provide an important piece of the puzzle in elucidating the role that each of the regions plays in the dynamic cortical network supporting the complex manual dexterity that is a hallmark of human evolution.

METHODS

Subjects

Three adult macaque monkeys (*Macaca mulatta*) were used in these studies. One male monkey (*monkey P*; 14 kg; 10–12 yr old during the course of the study) was used to examine the effects of deactivating area 5L of the posterior parietal cortex (PPC; Ref. 7) with a custom-made cooling device (see *Cooling Devices*; Ref. 71). One female monkey (*monkey A*; 9.3 kg; 11–13 yr old) and the other male monkey (*monkey M*; 13 kg; 5–9 yr old) were used to examine the effects of deactivating somatosensory area 2, primary motor cortex (M1), and area 7b of the PPC using either a "second-generation" cooling device (69, 70) or stainless steel cryoloops (56). All procedures were approved by the U.C. Davis Institutional Animal Care and Use Committee and conformed to National Institutes of Health guidelines.

Behavioral Training

All tasks involved a food reward, so monkeys were trained or tested in the morning and afternoon shortly before their usual feeding times. In addition to fruit, nuts, and other enrichment, monkeys worked primarily for one of two sizes of nutritionally balanced food pellets (Bio-Serv).

Monkeys were trained on two tasks; once they reached an average performance of 80% correct in all trial types in a primate chair without head restraint, a head holder was implanted (see *Surgeries*). After recovery, monkeys were gradually acclimated to head fixation during task performance. Once a postsurgical criterion of 80% was reached, monkeys underwent a second surgery during which the cooling devices were implanted over the regions of interest.

After the postoperative recovery period, monkeys were briefly tested on each task with a sham cooling to ensure that no gross deficits were present after cooling device implantation. Based on pilot experiments we decided to forgo extensive postoperative testing before beginning the cooling experiments as we were uncertain how long we would be able to consistently observe effects from cooling. Since no profound deficits were observed in these one or two postsurgical but precooling sessions, we decided to focus our analyses on our main comparisons of interest: within-session differences between baseline, inactivated, and recovery epochs (see *Data Analysis*). After recovery, cooling data were collected 5–7 days per week for two sessions per day.

Behavioral Tasks

Bimanual precision grip task.

This task required bimanual coordination and a precision grip to retrieve a food pellet. Data for this task were collected from *monkey P*. In this task the monkey lifted a vertically oriented cylinder with one hand to expose a food pellet that could then be grasped with a precision grip with the other hand (Fig. 2, *top*; see Ref. 35 for details). Before each trial, an experimenter raised the cylinder and placed a 1-g food pellet (diameter = 1.14 cm; Bio-Serv Dustless Precision Pellets) inside a small well within the cylinder. The experimenter then rotated the cylinder and lowered it into one of three well orientations (left, right, and center location conditions).

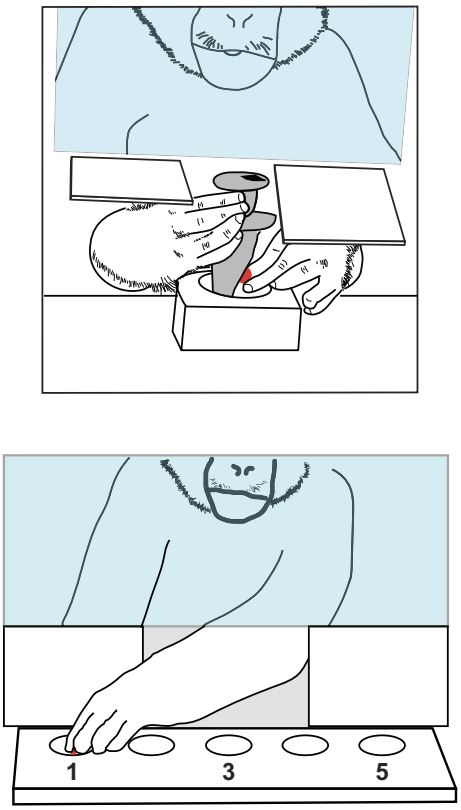

Figure 2. Behavioral tasks. *Top*: bimanual precision grip task. Monkeys reached through a pair of portholes covered by hinged doors to lift a centrally located cylinder (gray) with one hand and with the other hand retrieved a food pellet (red) from a well cut into the cylinder. The well was small enough to encourage use of a precision grip to access the pellet. The cylinder could occupy 1 of 3 location conditions: left (as shown), center (facing monkey), and right. When facing left or right, the task geometry forced the monkey to use the corresponding hand for retrieving and the opposite hand for lifting. In the center condition, either hand could be used for lifting or retrieving. Trials were conducted with and without visual feedback. During nonvisual trials, an opaque screen (not shown) was lowered to block the viewing window (light blue). Monkeys viewed the position of the cylinder before each trial began. *Bottom*: reach trajectory task. Monkeys reached through a central opening to 1 of 5 shallow wells to retrieve a food pellet (red). The size and position of the opening forced the monkey to use the contralateral hand to reach the peripheral wells (left hand for *well 1*, right hand for *well 5*). The monkey could use either hand to access the center well (*well 3*). Trials were conducted with or without visual feedback during reaching. During nonvisual trials, an opaque screen (not shown) was lowered to block the viewing window (light blue). Monkeys viewed the position of the treat before each trial began.

All of this took place so that the orientation of the well (and location of the pellet) was visible and known to the monkey before starting the trial. Trials took place in one of two visibility conditions: In the Visual condition, the viewing window remained unobscured throughout the entire trial. In the Nonvisual condition, a screen was lowered in front of the viewing window once the pellet location had been shown to the monkey. The monkey was then cued to maintain a starting position by depressing a pair of levers located on the monkey's side of the behavioral apparatus (inside the primate chair), one with each hand. After a variable delay period (0–4 s), a green LED was illuminated indicating the start of the trial. This cued the monkey to release the levers and reach each hand through a separate door to acquire the food pellet positioned in the well of the cylinder. If the monkey released either lever early, the trial was aborted and the experimenter prevented the monkey from entering the task workspace. The small size of the well prevented other grasp types (e.g., whole hand power grasp) from being used efficaciously. The monkey was free to choose which hand lifted the cylinder and which hand attempted the pellet retrieval. For the left and right cylinder orientations (location conditions), however, it was extremely difficult for the monkey to reach the well using the hand contralateral to the well, thus forcing the monkey to use the hand that matched the cylinder orientation to retrieve the pellet. To successfully complete the trial, the monkey had to lift the cylinder, grasp the pellet, and bring it back through the doors within 20 s. There were thus six conditions: two visibility conditions × three location conditions. These were alternated in pseudorandom order such that each was experienced within every set of six trials. In addition to reaction time (trial start until lever release), other measures included time for each door to open and close, time for the cylinder to be lifted and to fall, and treat possession latency. Door and cylinder latencies were measured with microswitches. Save for reaction time, all latency measures were calculated relative to lever release. High-definition video (1080p, 60 fps; Sanyo VPC-HD2000A Xacti or Canon VIXIA HF R500) was collected from a top-down angle centered on the cylinder, a second top-down angle behind the viewing window centered on the monkey's face, and a head-on angle facing the cylinder and monkey.

This task was designed specifically to examine the role that area 5L plays in reaching and grasping behavior (35). Although the hypothesized role that this region plays in reaching/grasping is less clear than the other regions we examined, previous studies showed increased firing of 5L neurons just before object contact (during grasp shaping) as well as during object manipulation, especially when a precision grip was used (17, 21–23, 72–74). Most importantly, we have found this task to be sensitive to permanent lesions of this region, whereas a more general reaching task and a texture discrimination task were not (35).

Reach task.

This task was used to assess gross motor ability as well as the use of the precision grip in a simpler context that was robust to changes in motivation. In addition, whereas success in the bimanual precision grip task relied mostly on fine digit coordination, this task primarily relied upon a successful reach trajectory. This task was used for *monkeys A* and *M*. An optically clear board (24 × 9 cm) with an array of five identical wells (6.8 mm deep) was fixed in front of a central opening (6 × 9 cm) configured such that the monkey could only use one hand at a time to reach and retrieve a 190-mg food pellet (Fig. 2, *bottom*; pellet diameter = 0.66 cm; Bio-Serv Fruit Crunchies). Three wells were used in this version of the task: left, center, and right (*locations 1*, *3*, and *5* of Fig. 2, *bottom*). The wells were narrow and deep enough that monkeys typically used a precision grip to retrieve the pellet, though they sometimes used whole hand "power grasp." The wells were still shallow enough that a poor reach trajectory could knock the pellet from the well, which was scored as a failure and the pellet was removed by the experimenter. The size of the opening also ensured that for the two lateral well positions the monkey was required to reach across its body from the contralateral side, thus forcing the monkey to use a specific hand for that position. The monkey could use either hand for the center position. A movable opaque screen in front of the viewing window allowed for retrieval with or without visual guidance.

Before the start of each trial, the experimenter placed a pellet in one of the wells and covered it with their finger. For the visual condition, the trial began when the experimenter's hand was removed. For the nonvisual condition, the screen was rapidly lowered, obscuring the monkey's vision. This closing of the screen signaled the start of the trial, and the experimenter simultaneously removed their hand covering the pellet. If the monkey began the trial early, the experimenter raised the screen and blocked access to the pellet until the monkey returned its hand through to its starting position. To successfully complete the trial, the monkey was required to remove the pellet from the well and bring it through the opening within 10 s without dropping it. As in the other task, visual and nonvisual trials were alternated and the pellet location pseudorandomly chosen such that each of the six conditions (2 visibility conditions × 3 location conditions) was experienced within every set of six trials. Video was collected from three angles: a head-on angle facing the task workspace, a bottom-up angle through the clear board to visualize both the pellet and the glabrous surface of the monkey's hand, and a top-down angle behind the viewing window centered on the monkey's face.

In addition to being robust to changes in motivational state resulting from inactivation of different cortical regions, the three different phases of this task (early reach, middle grasp, and late feeding) allowed us to test hypotheses about the potential function of our regions of interest as they relate to manual behavior. Beyond the actual movements required to successfully complete each phase, the ability to remove visual feedback during a trial allowed assessment of deficits related to touch and proprioception. Based on its hypothesized role in all aspects of complex movement (75–79), we predicted that cooling M1 would affect all phases of the task, regardless of visual feedback. Based on its hypothesized role in mediating proprioceptive monitoring of movements and assessing haptic information about the size/shape of grasped objects (74, 80–87), we predicted that cooling area 2 would similarly affect all phases of the task but the effects would be most pronounced when visual feedback was removed. Finally, based on its hypothesized role in controlling hand-mouth coordination and the goal of a given reaching/

grasping action (8, 32, 88), we predicted that cooling area 7b would preferentially affect the late phase of this task.

Task differences.

Although all three monkeys were initially trained to perform the bimanual precision grip task, pilot experiments revealed variability in the durability of a given cooling device as well as variability in each monkey's willingness to complete a complex task in the face of impairment. Initial efforts to interleave behavioral tasks in addition to cooling different regions yielded a relatively small amount of data per task and inactivation experiment. As such, we chose to focus on a single behavioral task in each monkey to maximize the amount of data per manipulation at the cost of a fully balanced design built around a classic double-dissociation of effects. Initially we had planned for the bimanual precision grip task to be the sole task each monkey was tested on, with additional tasks used for further testing once a full data set was collected for each cooled region. Preliminary testing with that task, however, revealed that it was difficult for monkeys to maintain motivation in the face of a more difficult task that required a relatively invariant sequence of starting positions and actions to automatically measure the latency of different task phases. To overcome this, we employed the reach task for the latter two experiments (*monkeys A* and *M*). Although the lack of onboard electronics precluded the type of precise latency measurements we could obtain with the bimanual task, it allowed the experimenter to manually control the progression through the task phases and quickly adjust to changes in the monkeys' motivation state.

Surgeries

After training to criterion, monkeys underwent an initial surgery in which either a standard cylinder-style head holder (*monkey P*; Crist Instrument Company, Hagerstown, MD) or an acrylic-free, fitted titanium head holder was implanted (*monkeys A* and *M*; Gray Matter Research, Bozeman, MT; see Ref. 89 for details). After head holder acclimation and training to criterion while head-fixed, each monkey underwent a surgery to implant cooling devices in several regions of interest in the hemisphere contralateral to the preferred hand. *Monkeys P* and *A* had cooling devices implanted in the right hemisphere, and *monkey M* received its implant in the left hemisphere. Before surgery, animals were induced with 30 mg/kg of ketamine hydrochloride (IM) and were maintained with isoflurane (1–2%). A craniotomy was made over parietal cortex, in two cases extending rostrally to expose motor and premotor cortices (*monkeys A* and *M*). After a durotomy, the cortical surface was imaged to relate blood vessel patterns and sulcal landmarks to cooling device placement (Fig. 3). Regions of interest were located by using landmarks such as the central, intraparietal, arcuate, and lateral sulci. For *monkey P*, area 5L was exposed by cutting the pia spanning the most lateral extent of the intraparietal sulcus, taking care not to damage any surrounding blood vessels. Although an attempt was made to place a cooling device in area 5L in each monkey, we often could not separate the banks of the IPS widely enough to accommodate a cooling device without risking serious damage to the blood vessels and potentially exsanguinating the adjacent cortex. Given that these monkeys underwent extensive training before surgery, we made the decision to only implant a sulcal probe if we felt we could open the IPS safely. As a result, we were only able to implant a cooling device in area 5L in one monkey (*monkey P*). After placement, cooling devices were secured to the surrounding dura with surgical glue and held in place with thin sheets of polydimethylsiloxane (PDMS) around the devices' periphery or the dura was draped over the margins of the devices and the dural sections were reattached to each other with either surgical glue or fibrin sealant (EVICEL, Ethicon). Temperature was monitored via microthermocouples (MTCs) implanted directly into the cortex (*monkey P*), at the cooling device-brain interface (*monkey A*), or at the cryoloop junction (i.e., where the loop comes back together and inflow/outflow tubing is parallel; *monkey M*). For all monkeys an acrylic skullcap was molded and placed over the craniotomy site and around the device tubing and MTC leads. Titanium bone screws were placed around the craniotomy to provide anchoring points for dental acrylic. A stainless steel implant chamber (diameter 3.35–4.35 cm) was then placed over the craniotomy site to protect the exposed ends of tubing and MTC leads. The chamber was secured with additional dental acrylic. Monkeys recovered for 1–2 wk before behavioral testing resumed.

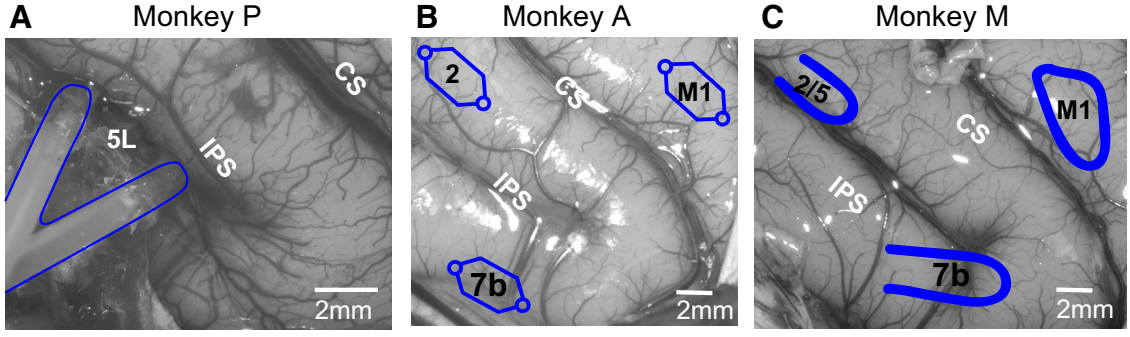

Figure 3. Cooling device placement: cooling chips (*A* and *B*) and cryoloops (*C*) were placed over cortical regions of interest for reversible inactivation. *A*: sulcal cooling device (with coolant tubes outlined in blue) implanted into the lateral aspect of the intraparietal sulcus (IPS) with the cooling surface facing area 5L (*monkey P*). *B*: outlines of coolant channels for devices placed over 3 regions: area 7b (*bottom left*), area 2 (*top left*), and M1 (*top right*) (*monkey A*). *C*: outlines of cryoloops placed over 3 regions: M1 (*top right*), area 7b (*bottom center*), and area 2/5M (*top left*) (*monkey M*). In *C*, the image was flipped for easier comparisons of device placement across monkeys. CS, central sulcus. IPS, intraparietal sulcus.

Cooling Devices

To examine the effects of deactivation of different cortical areas on manual behavior, we employed a method of transient inactivation via cortical cooling. This method allows for the deactivation of the cortex under and adjacent to the cooling device without affecting fibers of passage (see Ref. 54 for review). Extensive use of this technique by several groups has shown that neuronal activity is completely disrupted when the cortex is cooled below 20°C (e.g., Refs. 54, 71, 90, 91).

To cool area 5L, located in the rostrolateral portion of the intraparietal sulcus (7), *monkey P* was implanted with a "first-generation" sulcal cooling device (cooling "chip") inside the IPS as described in Ref. 71 (Fig. 2, E–H, of that article; Fig. 3*A* of the present article). The device comprised medical-grade silicone tubing (0.025-in. ID; A-M Systems, Sequim, WA) bent into a small loop (4 mm long × 5 mm wide) and embedded in a matrix of PDMS. PDMS on the caudal face of the device ensured that only the rostral bank of the sulcus was cooled to a temperature approaching deactivation threshold while the caudal bank was insulated (Fig. 8 in Ref. 71). Thus, we felt confident that any cooling spread to adjacent anterior intraparietal area (AIP) (in the caudolateral bank of the IPS, separated by VIP in the fundus; see Fig. 1 and Fig. 4*A*) was minimal. Temperature readings from the MTC implanted in the rostral bank of the intraparietal sulcus were used as the temperature feedback for the device (see *Cooling Device Control*).

Monkey A was implanted with second-generation gyral cooling devices (cooling chips) over areas 2 and 7b and primary motor cortex (M1) (Fig. 3*B*). All three devices cooled these regions from the gyral surface. As described previously (69, 70), these devices were comprised of a laser-etched PDMS microchannel attached to the cooling circuit via silicone tubing. For these devices, an MTC was attached to the bottom of the device to measure temperature at the device-cortex interface. This temperature was used as the feedback for controlling these devices.

Monkey M was implanted with stainless steel cryoloops as described in Ref. 56. Although our PDMS and silicone-based cooling devices were small, were easily insulated, and could be configured in a variety of sizes and shapes, they were not as robust to long-term usage in chronically implanted animals compared with the cryoloop design. Thus, to collect as much data as possible in this last monkey we elected to use cryoloops in lieu of the cooling devices used in *monkeys P* and *A*. These were implanted on the gyral surface over areas 2/5M and 7b and M1 as in *monkey A* (Fig. 3*C*). Temperature feedback for control of the cryoloops was measured via an MTC soldered to the inlet/outlet junction of the loop, as in Ref. 56.

It should be noted that the size, shape, and associated hardware (MTC leads and tubing) used in the second-generation cooling device used in *monkey A* differed from the cryoloops used in *monkey M*. Fitting three devices into a single craniotomy meant that there were a limited number of cooling site configurations that were possible, and as such, despite targeting the same regions in both monkeys, there was some variability in their exact placement within those regions (Figs. 3, 4). Similarly, differences in the materials/construction of the PDMS and silicone-based cooling devices used in *monkeys P* and *A* versus the stainless steel cryoloops used in *monkey M* meant that the temperature dynamics and overall cooling footprint differed between these experiments. Although cross validation of these different cooling techniques has not been performed, all three designs have been used successfully in published experiments (56, 68–71, 92).

Cooling Device Control

All devices were integrated into a "cooling circuit" that regulated the flow rate of the chilled ethanol through each device as described in Ref. 71. Thermocouple leads were connected to a TC-2000 thermocouple reader (Sable Systems). Both temperature and pump speed outputs were connected to a CED Power 1401 Mk II system (Cambridge Electronic Designs, Cambridge, UK), which implemented a custom algorithm to control pump speed (71). This algorithm adjusts the pump speed based on the trajectory of the temperature feedback during cooling.

For all monkeys, the target temperature was selected as follows. First, for each cooling device, pilot sessions were conducted to titrate to a behavioral effect. During these sessions, the device temperature was never set below 2°C, to ensure that no tissue was damaged. The highest temperatures that achieved qualitative behavioral disruption (e.g., abnormal hand postures, inaccurate reach trajectory) was chosen. Based on previous, acute cooling experiments (71), our data suggest that the inactivated regions were restricted to an area almost entirely below each cooling device. For *monkey P*, the MTC implanted in the rostral bank of the IPS (area 5L) was cooled to a target temperature of 20–25°C. Since this was the only monkey for which direct intracortical temperature measurements were collected, we chose this higher temperature range and confirmed via titration to behavioral effect. For *monkey A* the MTC placed at the interface of the cooling device and cortical surface was cooled to a target temperature of 10°C. For *monkey M*, the MTC built into the cryoloop junction was initially cooled to a target temperature of 5°C during the first few behavioral sessions for each area cooled. If no effect was observed at this temperature, subsequent sessions were conducted at a junction temperature of 2°C, as in Ref. 56. Differences in the materials and architecture of the gyral cooling devices used in *monkey A* and the stainless steel cryoloops used in *monkey M* likely accounted for the differences in target temperatures necessary to achieve a behavioral effect.

Cooling Sequence during Behavioral Testing

For all monkeys, task execution was broken into a set of three temperature epochs: Baseline, Inactivation, and Recovery (R1). In most instances, a fourth epoch (Recovery 2; R2) was conducted to determine whether any persistent deficits would abate given additional time (*monkey A* refused to work during this epoch in several sessions). The number of trials per epoch was chosen to balance satiation against having enough trials per condition to detect subtle behavioral effects. For the bimanual precision grip task this corresponded to 18 trials per epoch, resulting in 3 trials for each condition (2 visibility conditions × 3 location conditions × 3

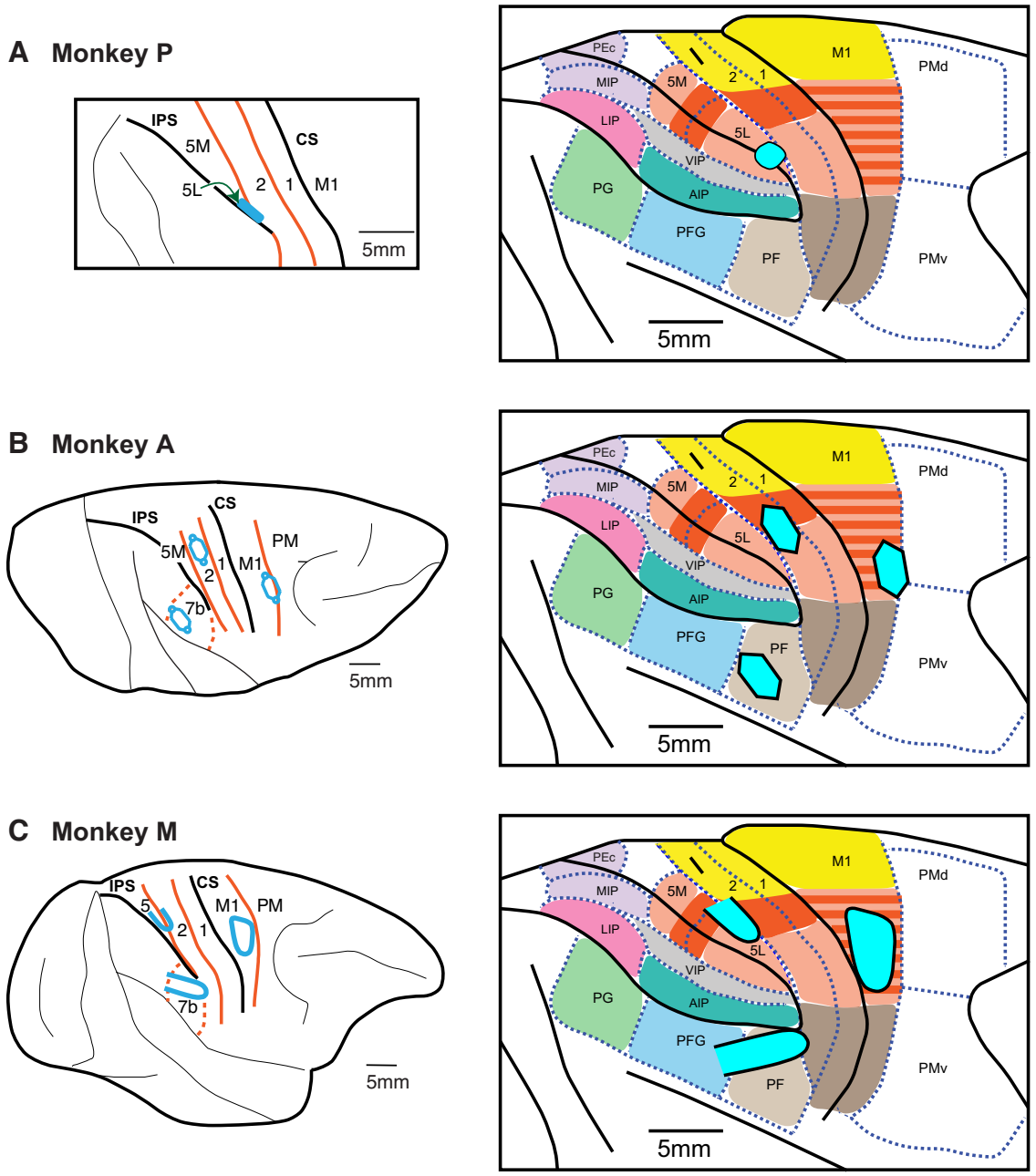

Figure 4. Histological reconstruction: the placement of cooling devices relative to cortical field boundaries (orange lines) determined from histologically processed tissue. Thick black lines (*left*) denote the intraparietal sulcus (IPS) and central sulcus (CS), whereas thin black lines (*left*) denote other sulci. *A*: a lateral view of portions of posterior parietal, anterior parietal, and motor cortex in *monkey P* in which a cooling device was placed on the rostromedial wall of the IPS, in area 5L. *B*: a dorsal view of the cortex of *monkey A* in which cooling devices were placed over M1, area 2 and area 7b. *C*: a lateral view of the cortex of *monkey M* in which cryoloops were placed over M1, area 7b, and area 2/5M. Note: cooling devices were implanted in the left hemisphere, but the image was flipped for easier comparisons of device placement across monkeys (as in Fig. 3). Images on *right* of each brain show the relative location of the cooling device with respect to functionally defined areas in motor cortex, anterior parietal cortex, and posterior parietal cortex. See Fig. 1 for details on functional definitions of cortical fields. It should be noted that the overall orientation of the brains in this figure differs from the orientation shown in the images in Fig. 3. but the relative size and orientation of the cooling chips between figures are the same. See Table 1 for abbreviations.

trials) per epoch. We used smaller pellets for the reach task, which allowed for 60 trials per epoch corresponding to 10 trials of each condition (2 visibility conditions $\times$ 3 location conditions $\times$ 10 trials).

The sequence of each session was as follows: After task execution at baseline temperature (Baseline epoch), the cortex was cooled to and held at target temperature for 5 min before the monkey began executing the tasks (Inactivation epoch). After the inactivation trials were complete, the pump was turned off and the cortex was allowed to rewarm for 5 min while the monkey was idle. Cooling device/brain temperature usually reached ~35°C within 2 min. Then the testing began again (Recovery; R1). For those sessions in which a fourth epoch was used (R2), an additional 5-min

break was given after the R1 epoch was over before the monkey was tested again.

During cooling, monkeys occasionally did not initiate trials. We designated these as "no-go" trials. For both tasks, we remained agnostic as to the reason behind no-go trials. These may have been due to general decreased motivation/aversion to working during cooling or a genuine impairment that left the monkey unwilling or unable to initiate a trial. Since there was no way to disambiguate these two scenarios, we analyzed the behavioral data in two sets: one in which no-go trials were counted as failure trials and one in which no-go trials were excluded from analysis.

Data Analysis

For each cooled area and task combination, performance was compared between temperature epochs in a set of two tests: Baseline versus Inactivation and Baseline versus Recovery (R1). Within each temperature epoch-based comparison, individual one-tailed Fisher's exact tests of task performance (see description for each task below) were analyzed for each lateral location condition (*wells 1* and *5* for reach task and cylinder locations left and right for bimanual precision grip task) and visibility condition (visual/nonvisual) combination in each task. One-tailed tests were performed under the hypothesis that for a given condition the Inactivation and Recovery epochs would yield worse performance compared with the Baseline epoch. We focused our analyses on the lateral locations, as trials involving the central position could be successfully executed by relying on the hand that was ipsilateral to the cooled region (since we never observed deficits of the ipsilateral hand/arm). We confirmed this via video analysis of hand choice for the central position in each task (see description for each task below). For each monkey, the hand contralateral to the cooled hemisphere was seldom or never used for the central position (*monkey A*, Supplemental Fig. S1; *monkey P*, Supplemental Fig. S2; all Supplemental Material is available at https://doi.org/10.6084/m9.figshare.14802675) or cooling induced a drastic reduction in its use (*monkey M*, Supplemental Fig. S1).

For the reach task, four tests per temperature epoch comparison were analyzed: well *locations L* and *R* for both visual and nonvisual trials (2 visibility conditions $\times$ 2 location conditions). With two comparisons (Baseline vs. Inactivation, Baseline vs. Recovery) this resulted in a set of eight tests per cooled region for each monkey. For each temperature comparison, the number of successful versus failed trials (combined across sessions) was analyzed in a 2×2 contingency table using Fisher's exact test and compared to a Bonferroni-corrected critical P value of $0.05/8 = 0.00625$. For this task the lack of onboard electronics precluded the precise measurement of trial completion latencies. To confirm hand choice in the central well location, hand use was scored for each trial at this location for those manipulations in which an effect was observed. As above, we compared the Baseline versus Inactivation epochs and the Baseline versus Recovery epochs. This involved a total of four tests per cooled region (2 visibility conditions $\times$ 1 location $\times$ 2 temperature epoch comparisons). For each temperature comparison, the number of trials (combined across sessions) using the hand contralateral versus ipsilateral to the cooled hemisphere was analyzed in a 2×2 contingency table using Fisher's exact test and compared to a Bonferroni-corrected critical P value of $0.05/4 = 0.0125$.

For the bimanual precision grip task, the use of a larger pellet size (which led to quicker satiation) resulted in fewer trials per epoch that could be collected compared with the reach task (18 vs. 60 trials per epoch). Comparisons between visual and nonvisual trials showed no statistically significant differences; therefore those trial types were collapsed to increase the number of trials per condition, yielding a total of two tests per temperature epoch comparison: cylinder location conditions left and right. This resulted in a set of four tests for *monkey P*. For this task, in addition to categorizing trials as success or failure, the latency from trial initiation (first hand removed from starting lever) until target possession (retrieving hand retracted from task workspace causing closure of door switch) was analyzed. If an otherwise successful trial's latency exceeded 2 standard deviations (SD range = 0.84–1.85 s across sessions) above the mean latency in the Baseline epoch for that session (mean range = 1.83–4.32 s across sessions), that trial was classified as "impaired." We omitted this additional layer of analysis for the reach task, since movements for that task were ballistic and generally were either successful on the first try or resulted in the pellet being knocked from the well.

For each temperature comparison, the number of successful versus failed/impaired trials (combined across sessions) was analyzed in a 2×2 contingency table using Fisher's exact test and compared to a Bonferroni-corrected P value of $0.05/4 = 0.0125$. We also compared just the trial completion latency measure described above independent of success measures, using the same set of four comparisons: Baseline versus Inactivation and Baseline versus Recovery for cylinder locations left and right. In addition, we also compared reaction times (time from trial start until the first hand was removed from starting lever), using the same set of four comparisons. In both cases, latency values were analyzed with a Wilcoxon rank-sum test and compared to a Bonferroni-corrected P value of $0.05/4 = 0.0125$. For these analyses, latency values from failed trials were not analyzed. Finally, as with the reach task, we confirmed hand choice for the central cylinder position by scoring hand use for those trials. We made the same temperature epoch comparisons as above for the one location, still collapsing visual and nonvisual trials (combined across sessions) together. This yielded two tests of ipsilateral versus contralateral hand use, each of which we analyzed in a 2×2 contingency table using Fisher's exact test and compared to a Bonferroni-corrected P value of $0.05/2 = 0.025$.

Video Analysis and Still Image Capture

All behavioral videos were time-synced and edited with Adobe Premiere Pro CC. For select trials, a sequence of frames (chosen at different time points within a trial to effectively summarize a behavior) was exported as a set of jpeg images. Images were cropped and adjusted for brightness and contrast with the use of Adobe Photoshop CC to maximize visibility of the hand and digits in each image. Some images were converted to grayscale to further increase visibility of the hand. Images were arrayed into sequences and

specific portions traced/labeled with Adobe Illustrator CC (Figs. 6–9 and 11–13).

Histology

To confirm the placement of the cooling devices and relate them to architectonic borders, monkeys were euthanized at the conclusion of the experiments with pentobarbital sodium (60 mg/kg IV) and then transcardially perfused with 0.9% saline followed by 4% paraformaldehyde in phosphate buffer and then 4% paraformaldehyde in 10% sucrose in phosphate buffer (pH = 7.4). The brain was removed from the skull, weighed, and photographed from multiple angles. After ~36-h immersion in 30% sucrose phosphate buffer, the brains were sectioned horizontally at 70 μm. Images of the tissue block face were taken before every section of the brain was cut. Alternate series of brain sections were stained for Nissl substance and myelin (93) and in one case SMI32 (31, 94). An entire series of sections was analyzed on a microscope, and cortical fields boundaries were drawn. The location of the cooling device was directly related to architectonic boundaries by matching blood vessels and sulci drawn in histologically processed sections with digital images of the exposed cortex before and after the implant and with the photograph taken after perfusion (Fig. 4).

RESULTS

We examined the manual abilities of three macaque monkeys using two different tasks: a reach and grasp task and a bimanual precision grip task. To determine the extent to which different cortical areas contribute to precise manual control, we reversibly deactivated primary motor cortex, anterior parietal area 2 (and in one case areas 2 and 5M), and posterior parietal areas 5L and 7 b (see Table 2 and Fig. 4 identifying the cortical locations of the cooling devices). Below we describe the effects of cooling different cortical areas on these tasks.

Reach Task

Area 2 and area 2/5M.

Figure 5 shows the success rate (successful trials/total trial number) for *monkey A* (Fig. 5, *left*) and monkey M (Fig. 5, *right*) in the reach task. We refined the analysis to the two lateral wells because these forced the monkey to use either the hand contralateral or ipsilateral to the cooling device. For conditions in which area 2 was cooled (Fig. 5*A*, *left*), *monkey A* showed a clear deficit when reaching with the contralateral hand in the nonvisual condition (dashed blue line) during the Inactivation (cooling) epoch (I) compared with the period immediately preceding the cooling (Baseline; B). This deficit persisted during the subsequent epoch when the cortex was allowed to return to normal physiological temperature (Recovery; R1). This level of performance continued to persist into the second Recovery epoch (R2). A smaller deficit was noted for the visual condition (solid blue line; epoch I). Both sets of deficits reached a Bonferroni-corrected significance criterion of $P < 0.00625$ (Fisher's exact test). Figure 6 and Supplemental Video S1 illustrate the types of cooling-induced kinematic changes responsible for this decrease in performance. Baseline behavior was characterized by fast and accurate acquisition of the pellet using a D1-D2 precision grip. Inactivation of area 2 often resulted in hypometric (undershooting) reaches that were exacerbated by removal of visual feedback, suggestive of a proprioceptive deficit. This is in contrast to the consistently high success rate in trials during which the monkey was forced to use the ipsilateral hand for both the visual (solid red line, Fig. 5*A*, *left*) and nonvisual (dashed red line) conditions.

When the experiment was repeated in *monkey M*, in which only a portion of the cooling device was over area 2 and the rest was over area 5M, this animal showed no deficits during inactivation. However, deficits were observed in contralateral hand performance during the Recovery (R1) epoch. These deficits manifested in both the visual (solid blue line) and nonvisual (dashed blue line) conditions (Fig. 5*A*, *right*) and were characterized by both hypometria and an exaggerated grasp aperture, as can be seen in Fig. 7 and Supplemental Video S2. Although not as severe as in *monkey A*, performance deficits reached statistical significance ($P < 0.00625$; Fisher's exact test) for both visually and non-visually guided reaches with the contralateral hand. These results indicate that area 2 is important for accurate reaching movements of the contralateral arm and hand.

Area 7b.

A similar analysis was conducted when these same monkeys underwent cooling of area 7b (Fig. 5*B*). In this case, there was a decrease in success rates in *monkey M* during the Inactivation (I) epoch when using the contralateral hand under both the visual (solid blue) and nonvisual (dashed blue) conditions (Fig. 5*B*, *right*; $P < 0.00625$; Fisher's exact test). Deficits typical of this manipulation were more heterogeneous compared with other regions that were deactivated but were often characterized by an exaggerated contralateral grip aperture in nonvisual trials and dropping of the pellet in both visual and nonvisual trials (Fig. 8; Supplemental Video S3). In addition, during visual trials the monkey often exhibited a behavior wherein it grasped the pellet with the affected hand but seemed to have difficulty opening the hand or bringing it to its mouth to consume it. Instead, it would use its unaffected hand to retrieve the pellet from the seemingly frozen grasp of the other hand. Behavior completely recovered once the cortex returned to normal temperature (R1). In contrast, *monkey A* showed no deficits during or after 7b cooling. However, the location of the cooling device was in a more lateral location than in *monkey M* and the cooling footprint was smaller.

Table 2. *Cortical cooling experiments: monkeys, areas cooled, and number of trials*

Monkey	Task	Area Cooled	Trials per Condition across All Sessions (by epoch)
A	Reach	Area 2	B, I, R1 = 68–70; R2 = 35–36 (7 sessions)
M	Reach	Area 2/5M	B, I, R1, R2 = 70 (7 sessions)
A	Reach	7b	B, I, R1, R2 = 40 (no effect; 4 sessions)
M	Reach	7b	B, I, R1, R2 = 110 (11 sessions)
A	Reach	M1	B, I, R1, R2 = 30 (no effect, 3 sessions)
M	Reach	M1	B, I, R1, R2 = 84–90 (9 sessions)
P	Bimanual	5L	B, R1, R2 = 41–52; I = 58–63 (6 sessions)

B, Baseline; I, Inactivation; R1, Recovery; R2, extended recovery.

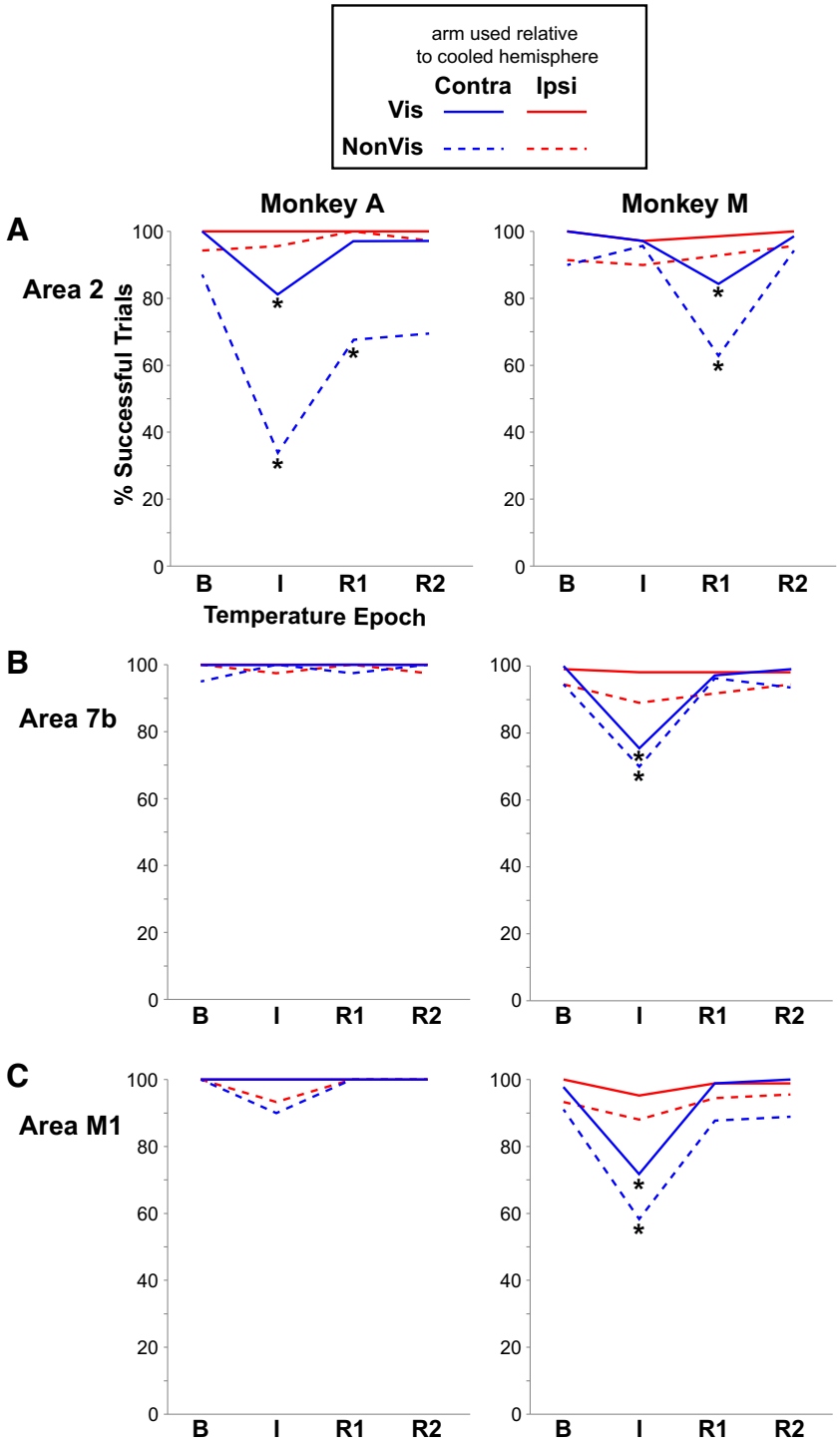

Figure 5. Reach trajectory task performance: percentage of successful trials during each temperature epoch (B, Baseline; I, Inactivation; R1, Recovery; R2, extended recovery) for each region cooled. Colored lines correspond to limb used (blue, contralateral; red, ipsilateral) and visibility condition (solid, visual; dashed, nonvisual). *A*: area 2 (2/5M in *monkey M*). *B*: area 7b. *C*: M1. Performance is shown for *monkey A* (*left*) and *monkey M* (*right*). Asterisks below data points denote statistically significant difference between the temperature epoch (I or R1) and Baseline for a given visibility/location condition by a Bonferroni-corrected Fisher's exact test ($P < 0.00625$). Cooling each region induced a profound deficit in 1 or both monkeys when the contralateral limb was used for reaching. Cooling area 2 (*A*) seemed to have the largest effect when visual feedback was removed. See Table 2 for number of trials per condition by temperature epoch.

Motor cortex.

Finally, a third cooling device was implanted over motor cortex (M1) in both monkeys (Fig. 5*C*). Cooling this region induced a significant deficit in *monkey M* for both visual and nonvisual trials in which the contralateral hand was used (Fig. 5*C*, *right*; $P < 0.00625$; Fisher's exact test). Unlike cooling anterior or posterior parietal cortex, motor cortex cooling produced both a severe reaching and grasping deficit characterized by hypermetria (overreaching) and an inability to close the hand when the grasp would normally be initiated, leading to a splayed posture that hovered over the pellet and often drifted toward the body's midline (Fig. 9; Supplemental Video S4). When the pellet was successfully grasped with the affected hand, the monkey often employed the same feeding strategy used during 7b cooling, removing the pellet from the affected hand's grasp and feeding itself with the unaffected hand. As with 7b, these deficits disappeared once cortex returned to normal temperature.

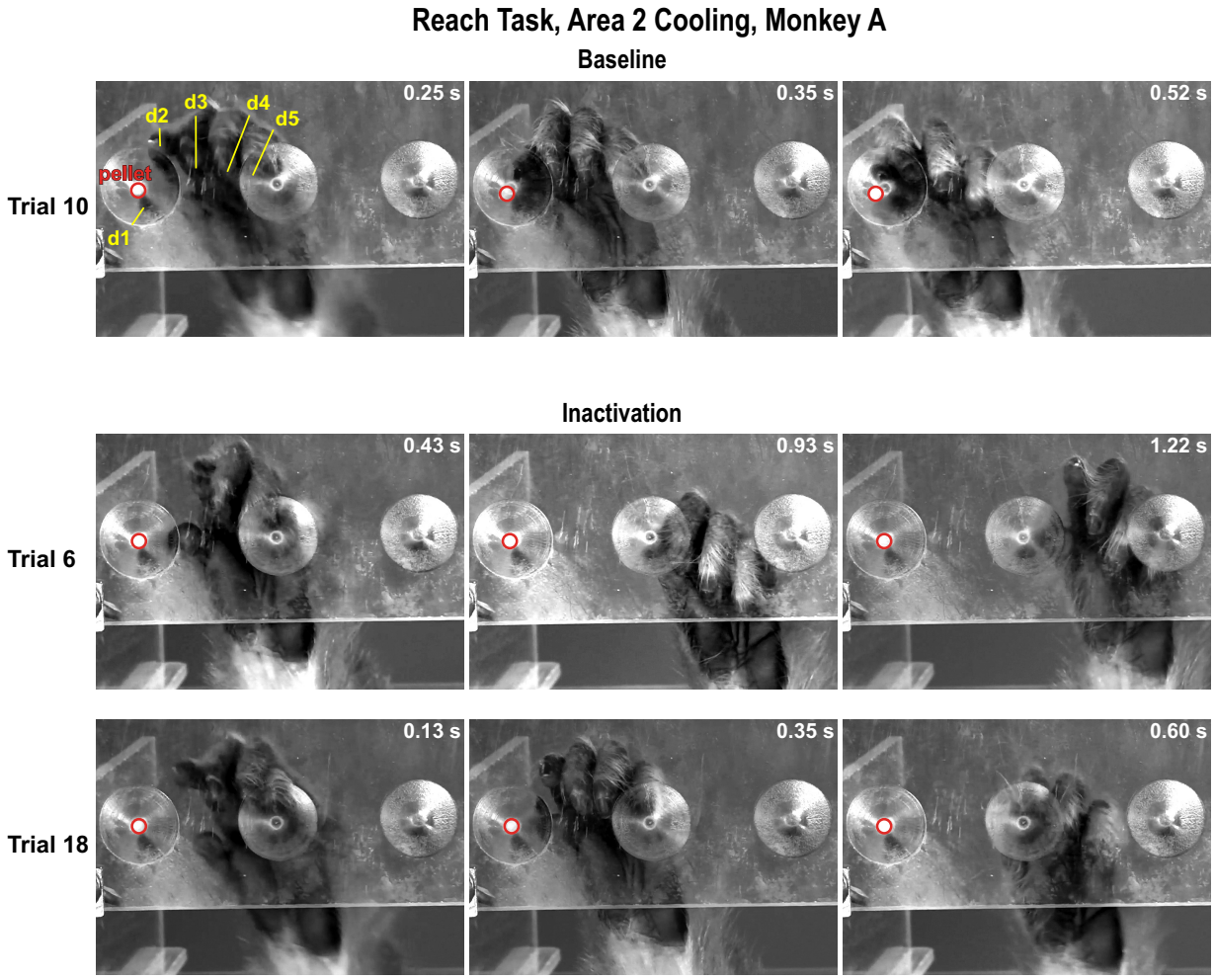

Figure 6. Reach trajectory task (area 2 cooling, *monkey A*): still frames captured from below the wells showing the pellet (outlined in red) and the glabrous surface of the monkey's hand with each digit labeled (yellow). Time after movement initiation is given in the corner of each frame. Trial number of corresponding epochs is shown on *left* of each row of frames. During a Baseline epoch trial (*top*), the monkey easily grasped the pellet with the hand contralateral to the cooled region with a D1-D2 precision grip. During 2 Inactivation epoch trials (*bottom*), reaches were hypometric (lateral undershoot going left) and drifted toward the monkey's midline (missing the pellet and going rightward).

Cooling motor cortex in *monkey A* did not produce any consistent effects once data collection was initiated. During a pilot session when motor cortex was cooled for the first time, *monkey A* exhibited hypometric reaches with the contralateral hand during nonvisual trials. These deficits were similar to those evoked by cooling area 2. However, this effect could not be reproduced in subsequent sessions. Although the cooling device was mostly over motor cortex, a portion of the device was also in PM. In addition, compared with *monkey M* the footprint of the device was smaller.

The preceding analyses were conducted with all possible trials included, including those in which the monkey did not initiate a reaching movement (no-go trials). Given that we rarely if ever saw this type of response in the Baseline condition, we reasoned that this could be due to the fact that the monkey simply was unable to move the limb and/or plan the appropriate movement. Alternatively, the monkey may have lost motivation, or there may have been some other nonmotor deficit that was induced by either the cooling or the time period that the monkey was working. This behavior was almost always seen in trials involving the limb contralateral to the cooled hemisphere during either the Inactivation or first recovery epoch (Recovery 1), especially during nonvisual trials, and seemed to roughly correlate with the monkey's level of impairment resulting from cooling. It also became less common as more sessions were conducted, suggesting that it was not a result of increasing damage or decreasing motivation over time. Excluding these trials from the analyses slightly reduced the effect sizes for certain conditions (data not shown), but the statistical significance was not changed.

Bimanual Precision Grip Task: Area 5L

Monkey P was trained on the bimanual precision grip task, in which they were required to lift a cylinder with one hand and retrieve a food pellet with the other hand using a precision grip. The location of the food well was varied for each trial such that it was only possible to retrieve it with the contralateral hand, the ipsilateral hand, or either hand (center position). The results combined across the nonvisual and visual conditions are shown in Fig. 10*A* for trials requiring

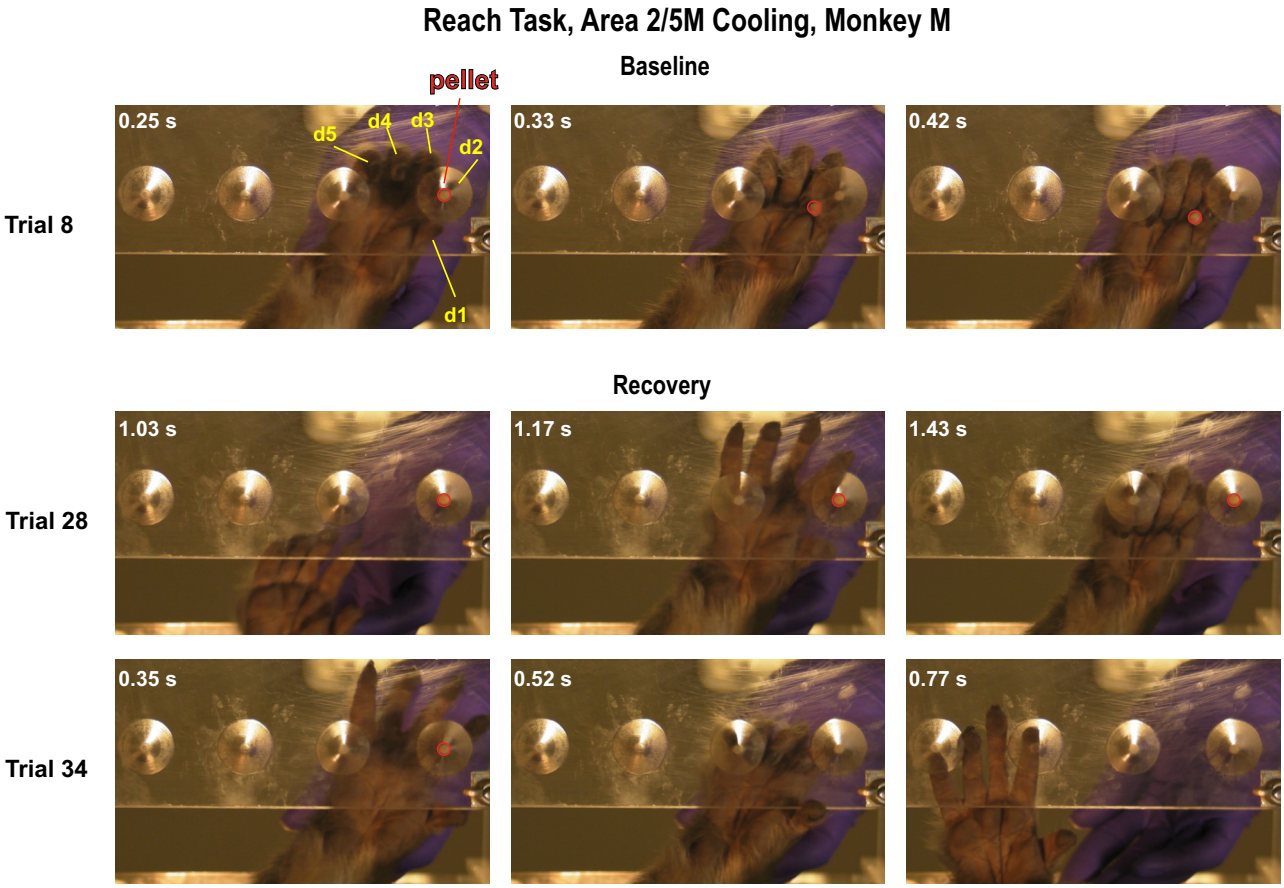

Figure 7. Reach trajectory task (area 2 cooling, *monkey M*): as with *monkey A*, during the Baseline epoch (*top*) the monkey easily grasped the pellet (outlined in red when present) with the hand contralateral to the cooled region with a D1-D2 precision grip. During the Inactivation epoch (not shown) no deficits appeared. During the Recovery epoch (*bottom*, 2 trials shown), however, reaches were hypometric (lateral undershoot going right) and showed little preshaping of the hand. Note that pellet has been dislodged from well in *center* and *right* frames of *trial 34*. Conventions as in Fig. 6.

the contralateral hand (blue line) or the ipsilateral hand (red line) for pellet retrieval. These results show the percentage of trials that the monkey was successful and completed the trial at a speed that was not significantly slower (mean + 2 SDs) than during the Baseline (uncooled) temperature epoch for that location condition. This allowed us to account for trials in which a deficit was present but not severe enough to result in a failed trial. Figure 10*B* shows the same data, but only comparing successful versus failed trials. Although baseline performance was characterized by a high success rate by both behavioral measures, cooling area 5L induced a deficit for both the contralateral (blue line) and ipsilateral (red line) well positions. The deficit for both well positions was due to impairment of the contralateral hand rather than an impairment of both the contralateral and ipsilateral hands. Indeed, since this is a bimanual task, deficits in using the contralateral hand could manifest during pellet retrieval (when the pellet faced the contralateral side) or holding the cylinder itself (when the pellet faced the ipsilateral side). As shown in Fig. 11 and Supplemental Video S5, whereas baseline pellet retrieval with the contralateral hand was typified by a preshaped hand culminating in a D1-D2 precision grip, cooling often resulted in an open-handed posture in which D1 and D2 encircled the cylinder rather than the pellet. When a precision grip could be executed, the monkey often failed to firmly grasp and pick up the pellet, despite its fingers being in the correct position. Figure 12 and Supplemental Video S5 illustrate the effects when the contralateral hand was used for cylinder holding such that the ipsilateral hand retrieved the pellet. In the Baseline condition a preformed grasp quickly encircled the cylinder and maintained it at a height that allowed access to the pellet. In contrast, during cooling the hand approached the cylinder in a limp posture and remained open for an extended period before closing (if it did so at all). Even once closed around the cylinder the contralateral hand often failed to maintain it at the proper height for retrieving the pellet. At times, the severity of impairment to the contralateral hand was such that even entering the task workspace was affected. Figure 13 and Supplemental Video S5 illustrate this deficit. Although baseline behavior was characterized by swift removal of the contralateral hand from the starting lever and unimpeded entry through the porthole, cooling often caused inaccurate hand trajectories that resulted in collisions with the viewing window.

Although the effects described above were dramatic, idiosyncrasies in their onset (see DISCUSSION) combined with a low number of trials per condition limited the statistical significance of the results with our conservative Bonferroni-corrected criterion ($P < 0.0125$). Nevertheless, as seen in Fig.

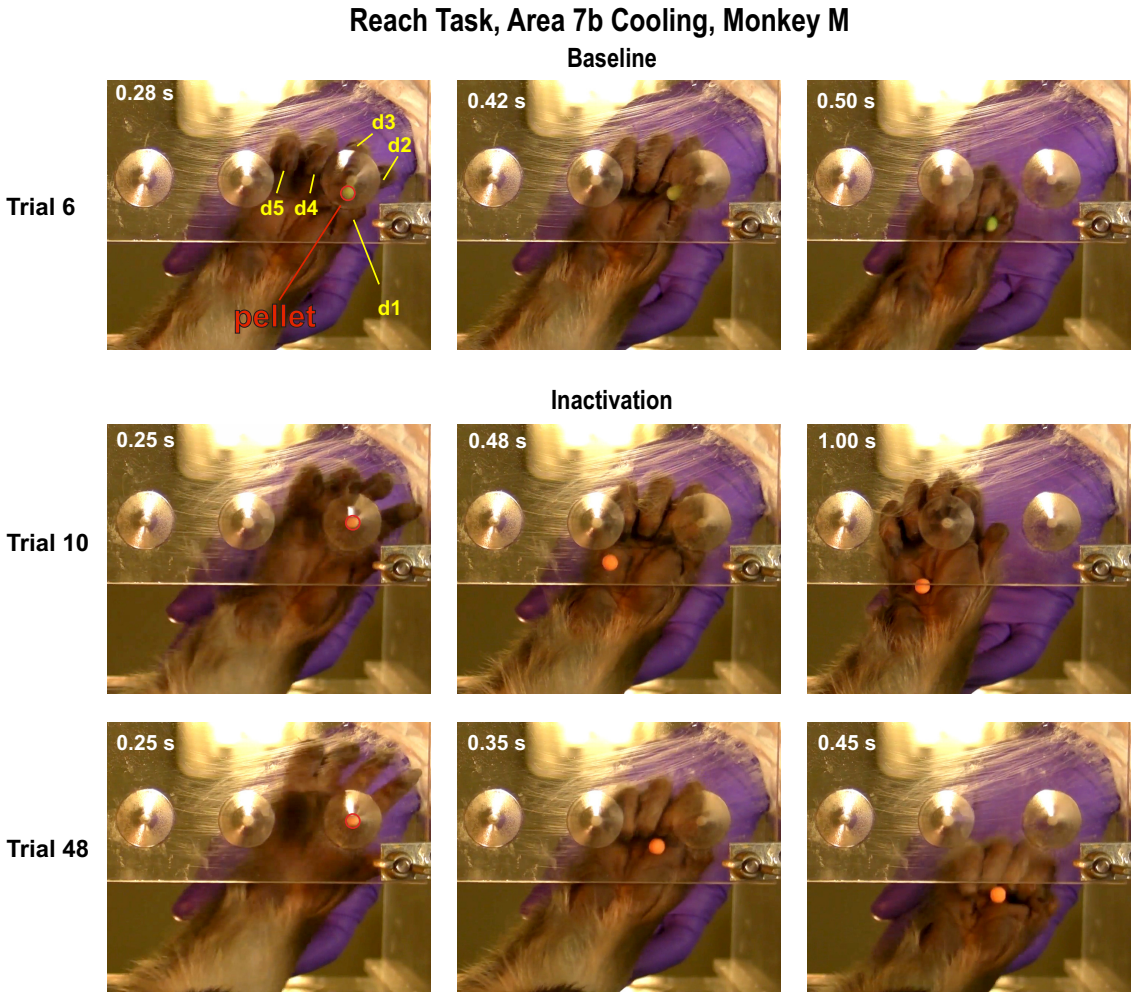

Figure 8. Reach trajectory task (area 7b cooling, *monkey M*): like the baseline epoch shown in Fig. 7, the Baseline epoch (*top*) was characterized by accurate reaches using a D1-D2 precision grip with the hand contralateral to the cooled region (pellet outlined in red for the first frame of each trial). During Inactivation (*bottom*, 2 trials shown), deficits were heterogeneous but often included an exaggerated grip aperture that dislodged the pellet; pellets that were grasped were often dropped. Conventions as in previous figures.

10*A* the proportion of trials in which the monkey exhibited no difficulty (successful trial that was not 2 SDs slower than the mean) was significantly lower for ipsilateral-facing trials (contralateral hand used for cylinder lifting) and was nearly significant for contralateral-facing trials (contralateral hand used for pellet retrieval). Figure 10*B* shows the same data, but only comparing the rate of successful versus failed trials. Note that this renders the effect of ipsilateral-facing trials statistically insignificant, while leaving contralateral-facing trials largely unchanged. This highlights the importance of examining both the rate of success and the task completion latency in successful trials in capturing the effects of cooling. When task completion latency for successful trials was analyzed separately, we found significant slowing in ipsilateral-facing trials during inactivation, which was the main source of difficulty in these trials rather than total failure (Supplemental Fig. S3). Analysis of reaction times of successful trials did not yield any significant differences between epochs (Supplemental Fig. S4). In the Recovery epoch, performance increased to be statistically indistinguishable from Baseline, although some deficits persisted (Fig. 10*A*). When only success rate was measured, the contralateral-facing condition saw deficits persist into the Recovery periods (Fig. 10*B*), although any persistent deficits had abated by the next testing session.

As with the behavioral analysis of cooling other regions during the reach task, Fig. 10 reflects performance including trials in which the monkey would not initiate a movement (no-go trials). These trials followed a similar pattern as in the reach task: they almost always occurred during use of the limb contralateral to the cooled hemisphere, especially during nonvisual trials in either the Inactivation or first Recovery epochs. As with *monkeys A* and *M*, they also became less frequent over subsequent sessions. As with the reach task, we also analyzed performance with these trials excluded. Given that this reduced the number of trials, the effect size of our manipulations was diminished (though statistical significance remained unchanged). Regardless, the same trends shown in Fig. 10 were robust to the removal of these trials: cooling area 5L resulted in a deficit in use of the contralateral hand that manifested primarily as failed trials when it was used for pellet retrieval and as slower trials

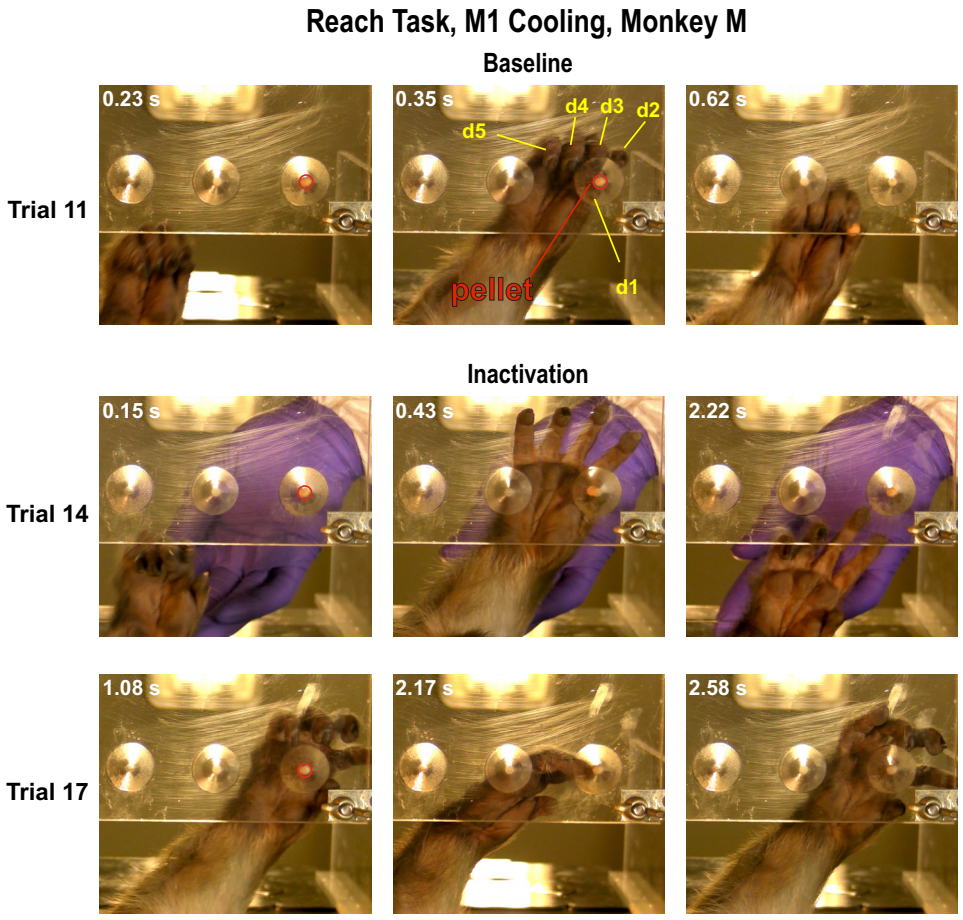

Figure 9. Reach trajectory task (M1 cooling, *monkey M*): as in previous figures, the Baseline epoch (*top*) was characterized by accurate reaching and grasping with a precision grip. During Inactivation (*bottom*, 2 trials shown) severe reaching and grasping deficits were observed: a hypermetric (overshooting) reach and splayed, open hand posture that often drifted toward the body's midline.

when it was used to hold the cylinder. As in the previous analysis, the Recovery periods saw reduced performance compared with the Baseline epoch (though not statistically significantly lower).

Limitations and Technical Considerations

There were several findings that should be considered when interpreting our results. First, in *monkey M* we observed no deficits during the cooling of area 2. Rather, the deficits that emerged only did so once the cortex was rewarmed. Previous work by our laboratory (69, 70) and others (95, 96) has shown that rewarming neural tissue after cooling can lead to "rebound" excitability. Thus, it is possible that although the perturbation induced by cooling area 2/5M was not enough to evoke deficits, the perturbation induced by rewarming was. This also may explain why some of the deficits we observed persisted into the Recovery epoch later in the session but not into the Baseline epoch on the next session of testing (Supplemental Fig. S5).

Second, in each of the three monkeys we observed granulation tissue growing between the cooling devices and the targeted cortex. This left us a window of time (~60–90 days) that, although markedly longer than that afforded to us by lesions, nonetheless placed limits on how long our devices produced observable effects. We believe this may be why we observed effects following cooling of 7b and motor cortex in *monkey M* but not *monkey A* (although we did see an effect during cooling of M1 in this monkey, but only for the first session). Even for those regions where we did observe effects, only a limited amount of data could be collected. We also felt it was important to employ somewhat naturalistic tasks in which the target object (food pellet) was also the monkey's reward, thus limiting the number of trials we could conduct before satiation set in. This limit on both the number of trials within a session and the number of sessions overall likely prevented more subtle deficits from reaching statistical significance.

Finally, it should be noted that some of the differences we observed between monkeys likely had to do with differences in the behavioral task (*monkey P* tested with the bimanual precision grip task vs. *monkeys A* and *M* tested with the reach task; see *Task differences*) as well as the exact placement of the cooling devices, which targeted the same regions in different monkeys (*monkey A* vs. *monkey M*). In addition, we were only able to successfully implant a cooling device in area 5L in one monkey (see *Surgeries*). These factors do place limits on the conclusions we can draw from this investigation.

DISCUSSION

We reversibly inactivated several regions in the fronto-parietal reaching and grasping network independently while monkeys performed two different manual tasks: one focused on reach trajectory to acquire a free-standing target and another focused on both bimanual coordination and fine use

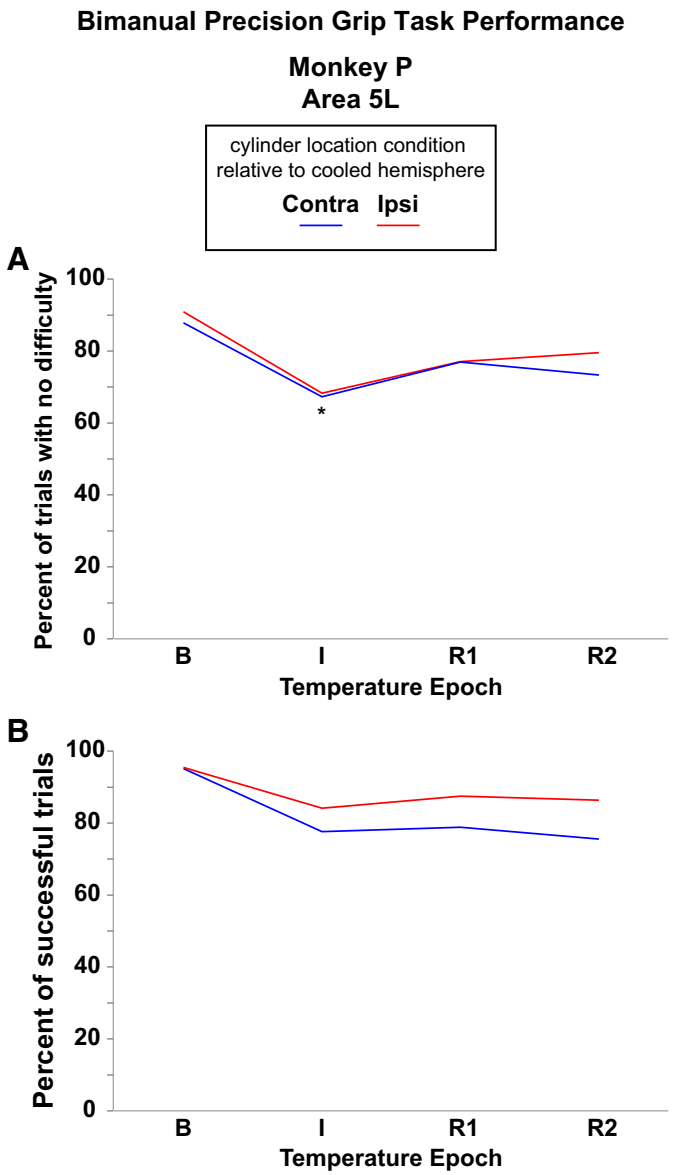

Figure 10. Bimanual precision grip task performance: *A*: percentage of trials with no difficulty (successful trial that was not 2 SDs slower than the mean). *B*: percentage of successful trials during each temperature epoch (B, Baseline; I, Inactivation; R1, Recovery; R2, extended recovery) for cooling area 5L in *monkey P*. Colored lines correspond to location condition of the cylinder's food well and thus the hand required for grasping the pellet (blue, contralateral to the cooled region; red, ipsilateral to the cooled region), collapsed across visibility condition. Asterisks below data points denote statistically significant difference between the temperature epoch (I or R1) and Baseline for a given location condition by a Bonferroni-corrected Fisher's exact test ($P < 0.0125$). Although baseline performance was characterized by a high success rate by both behavioral measures, cooling area 5L induced a deficit for both the contralateral (blue line) and ipsilateral (red line) well position. See Table 2 for number of trials per condition by temperature epoch.

of the digits to extract an object from a small space. Our results indicate that the different areas tested form a complex network of motor control that is overlapping, but several consistent themes emerged that suggest the independent roles that motor cortex, area 2, area 7b, and area 5L play in the different phases of reaching and grasping behavior. Cooling motor cortex produced a generalized set of deficits that affected nearly every stage of reaching and grasping regardless of whether the monkey had visual feedback, with the most severe deficits manifesting as a splayed hand posture that would not close around the pellet. Cooling area 2 resulted in a set of behaviors suggestive of deficits in proprioception: hypometric reaches and exaggerated grip apertures that were most pronounced during trials lacking visual feedback. Cooling area 7b produced a more heterogeneous set of deficits that nonetheless skewed more heavily toward the later stages of target acquisition: dropping the pellet once grasped or an inability to open the affected hand or bring the pellet to the mouth. Much like cooling area 7b, cooling area 5L also produced a somewhat heterogeneous set of deficits. In contrast to cooling area 7b, however, cooling area 5L produced deficits that skewed more toward early and middle stages of target acquisition: difficulty navigating the hand into the task workspace, improper apposition of the thumb and forefinger (D1 and D2) when retrieving the pellet, and a slack, open-handed posture when lifting the cylinder. Thus, despite the limitations of this study, we provide evidence for a motor planning and execution network wherein area 5L is involved in early stages and area 7b the later stages of a reaching and grasping movement, motor cortex is involved in all aspects of the execution of the movement, and area 2 provides proprioceptive feedback throughout the movement.

The present study builds upon a rich foundation of both electrophysiological and loss-of-function studies to provide a more complete picture of the roles played by different regions in the fronto-parietal reaching and grasping network during manual behavior. Importantly, this is the first study to deactivate area 7b or area 5L in isolation as well as the first to deactivate portions of area 2 and M1 with a method with high temporal resolution (on the order of minutes). As detailed below, previous studies largely relied on either irreversible techniques (lesions) or those that operate on longer timescales of onset and offset (e.g., muscimol). Although some of those studies have made use of cooling to deactivate portions of the fronto-parietal reaching and grasping network, they either inactivated large regions of cortex that included but were not restricted to these regions or inactivated different regions altogether. In addition, this study is the first to directly compare the results of cooling motor cortex, anterior parietal cortex, and posterior parietal cortex in the same animals. Finally, although ours is not the first to employ reversible inactivation to study the effects on retrieving small food items from recessed wells (e.g., Refs. 87, 97, 98), ours is the first to employ a bimanual reaching and grasping task in such a context. Furthermore, our tasks are complex yet ethologically relevant, as monkeys commonly retrieve small items of interest, either uni- or bimanually, whereas many studies concentrate on simpler or abstracted reaching and grasping tasks. Thus, selective inactivation and reactivation within the same behavioral session of discrete nodes in this network, coupled with a complex yet straightforward pair of motor tasks, has allowed us to better refine the roles of these areas in purposeful reaching and grasping under both visually guided and non-visually guided conditions.

In the following discussion, we review previous studies that examined the functional results of deactivating or

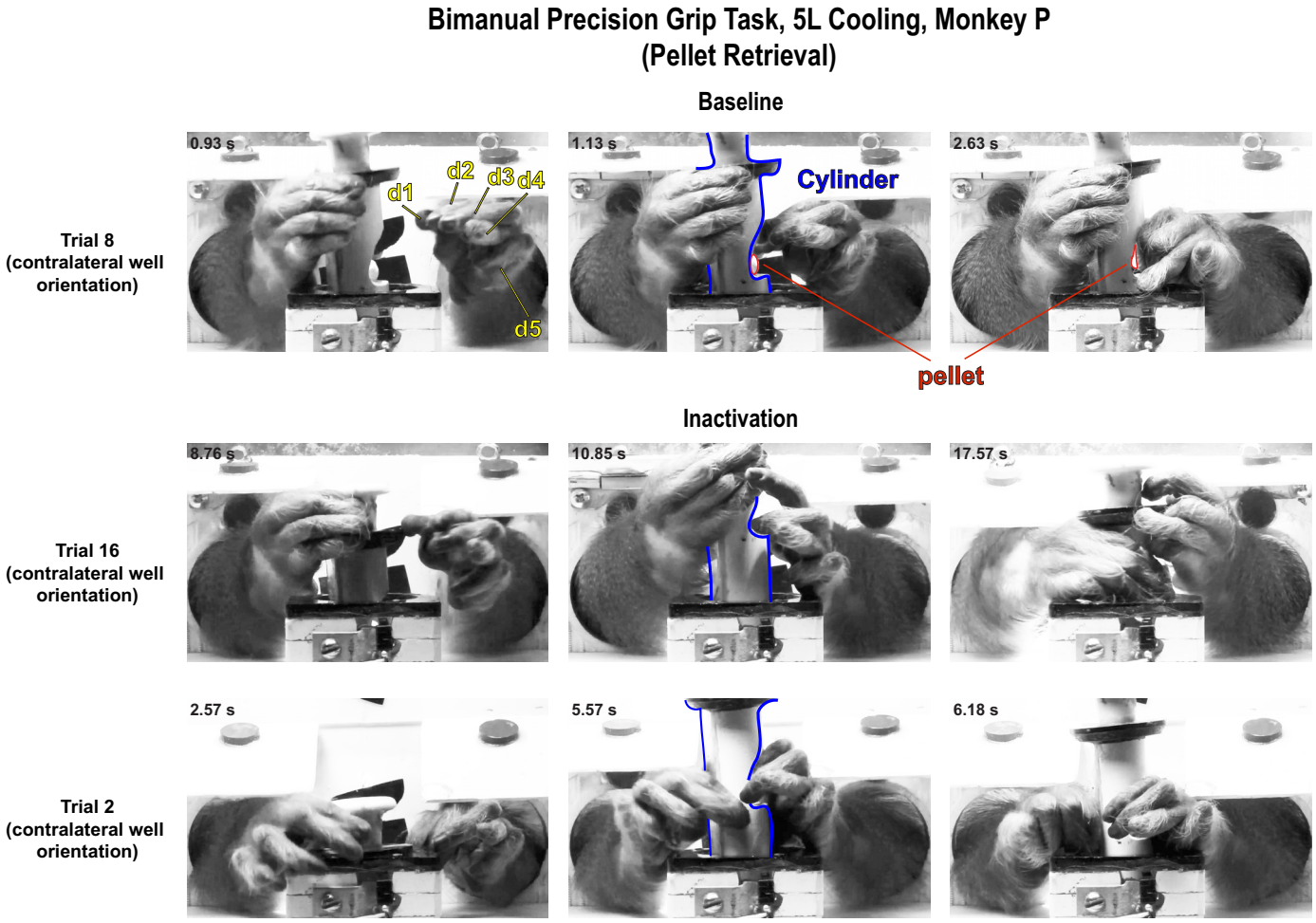

Figure 11. Bimanual precision grip task (*monkey P*, area 5L cooling; pellet retrieval by the affected hand): still frames from a head-on angle showing the pellet (outlined in red), the 5 digits of the hand (labeled in yellow), and the cylinder (outlined in blue). The monkey had to lift the cylinder with one hand, hold it, and retrieve the pellet with the opposite hand. The labeled hand retrieving the pellet is contralateral to the cooled region. During the Baseline epoch (*top*), the monkey easily retrieved the pellet with a D1-D2 precision grip. During the Inactivation epoch (*bottom*, 2 trials shown), the monkey used an open-handed posture, often encircling the cylinder rather than the pellet. Well orientation (facing contralateral hand) listed under trial number. Conventions as in Figs. 6–9.

lesioning portions of the fronto-parietal reaching and grasping network and compare these to our own data. Some differences between our results and those of previous investigations likely reflect the fact that most of our experiments focused on areas found on the gyri of parietal and frontal cortex while several reaching and grasping areas beyond 5L located in the IPS (namely the anterior and medial intraparietal areas) were not explored in this study. Although constraints on implant geometry and surgical outcomes limited the number of regions we could investigate in each animal, this study nevertheless makes important contributions to the field: *1*) the targeted inactivation of specific regions within posterior parietal cortex that have never been studied without involving adjacent fields; *2*) inactivation of different areas in the fronto-parietal reaching and grasping network in the same animals while the animals perform ethologically relevant tasks; *3*) employing a method of inactivation with a high enough temporal resolution to visualize both deficits and recovery within the same behavioral session; and *4*) complimenting the wealth of electrophysiological investigations of this network with functional assessment beyond thoroughly studied regions such as LIP and PRR.

Motor Cortex

We placed our cooling devices over the expected location of the hand representation in M1 as defined previously in our laboratory with intracortical microstimulation techniques (Fig. 4; Ref. 99). Our results were consistent with previous studies that deactivated a similar region in M1. For example, muscimol-based inactivations that overlap this region (87, 100, 101) evoke a hypotonia and paresis during reaching and grasping as well as the loss of independent finger movements. Perhaps most significantly, the "flat" hand posture described by Fogassi et al. (101) is quite similar to the "splayed" hand posture we observed during the initial reach. Although we did not measure grip forces as part of this task, the monkey's frequent inability to completely close its hand or fingers around the pellet is largely in accord with these previous results. This hand posture may also reflect a decrease in

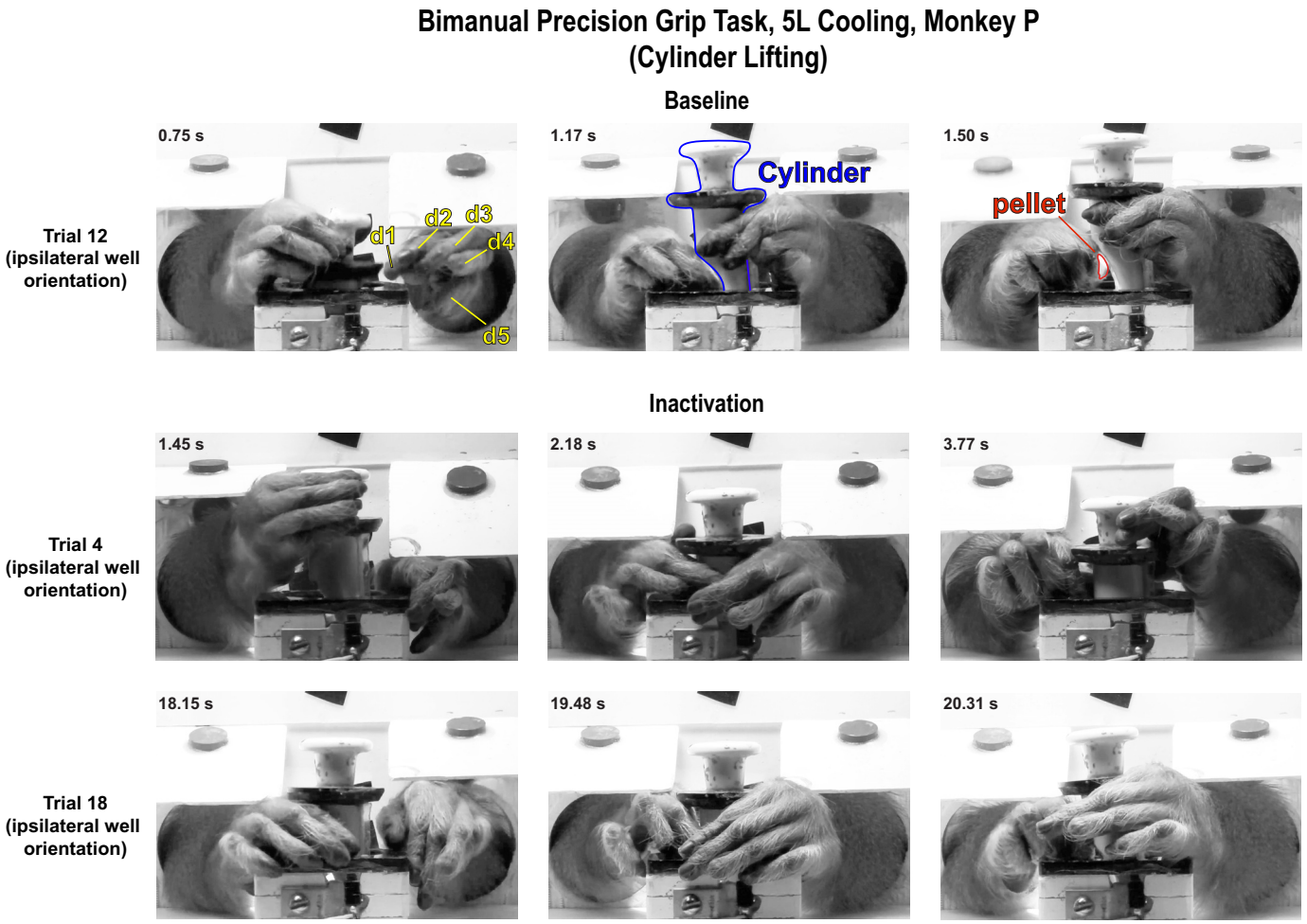

Figure 12. Bimanual precision grip task (*monkey P*, area 5L cooling; cylinder lifting by the affected hand): same conventions as Fig. 11 but with the labeled hand (contralateral to cooled region) lifting and holding the cylinder while the opposite hand retrieved the pellet. During the Baseline epoch (*top*), the monkey lifted and maintained the cylinder at an appropriate height, allowing the opposite hand to retrieve the pellet. During the Inactivation epoch (*bottom*, 2 trials shown), the monkey used a limp, open-handed posture pressed against the cylinder without necessarily gripping it. When a grip was used, the proper height often was not maintained. Well orientation (facing ipsilateral hand) listed under trial number. Conventions as in Fig. 11.

the ability to use the individuated finger movements necessary to execute a D1-D2 precision grip. Interestingly, the monkey's frequent inability to open its hand if it did successfully grasp the pellet suggests a possible hypotonia of digit extensors in addition to flexors. Overall, our results confirm previous work while affording a greater temporal resolution of effect than muscimol and avoiding the reorganization and confounds associated with permanent lesions: M1 seems to be involved in all stages of reaching and grasping, regardless of whether visual feedback is removed. This is consistent with a recent study in our laboratory in anesthetized macaques that demonstrates that cooling M1 had a large, global impact on evoked movements in areas 5, 7a, 7b, and 2 (102). This highlights the fact that although movement-related activity can be found throughout parietal cortex, M1 represents a key node of convergence of motor actions by virtue of its dense corticospinal connections (103–106).

Area 2

Our goal for cooling area 2 was to inactivate a somatosensory cortical region involved in proprioception and compare that to inactivation of motor cortex and posterior parietal cortex. Because neurons in area 2 have relatively large receptive fields and more complex response properties compared with somatosensory areas 3b and 1 (e.g., Refs. 81, 107–109), as well as its dense connections with portions of area 5 (27, 110–112), area 2 could be considered the most "PPC like" of the somatosensory cortical regions located in anterior parietal cortex (see Ref. 6 for review). In placing our cooling devices, our goal was to inactivate representations of both the hand and forelimb such that both reaching and grasping might be disrupted. Histological reconstruction confirmed that for *monkey A* our cooling device was confined to area 2, whereas in *monkey M* the cryoloop partially overlapped both area 2 and area 5M. This difference in placement may account for some of the differences in effects we observed between the two monkeys, with *monkey M* only exhibiting deficits during the Recovery epoch.

Early work examining the effects of relatively large lesions of the hand and forelimb representations of area 2 described deficits related to texture discrimination (84) as well as deficits in discriminating object properties such as angles, size,

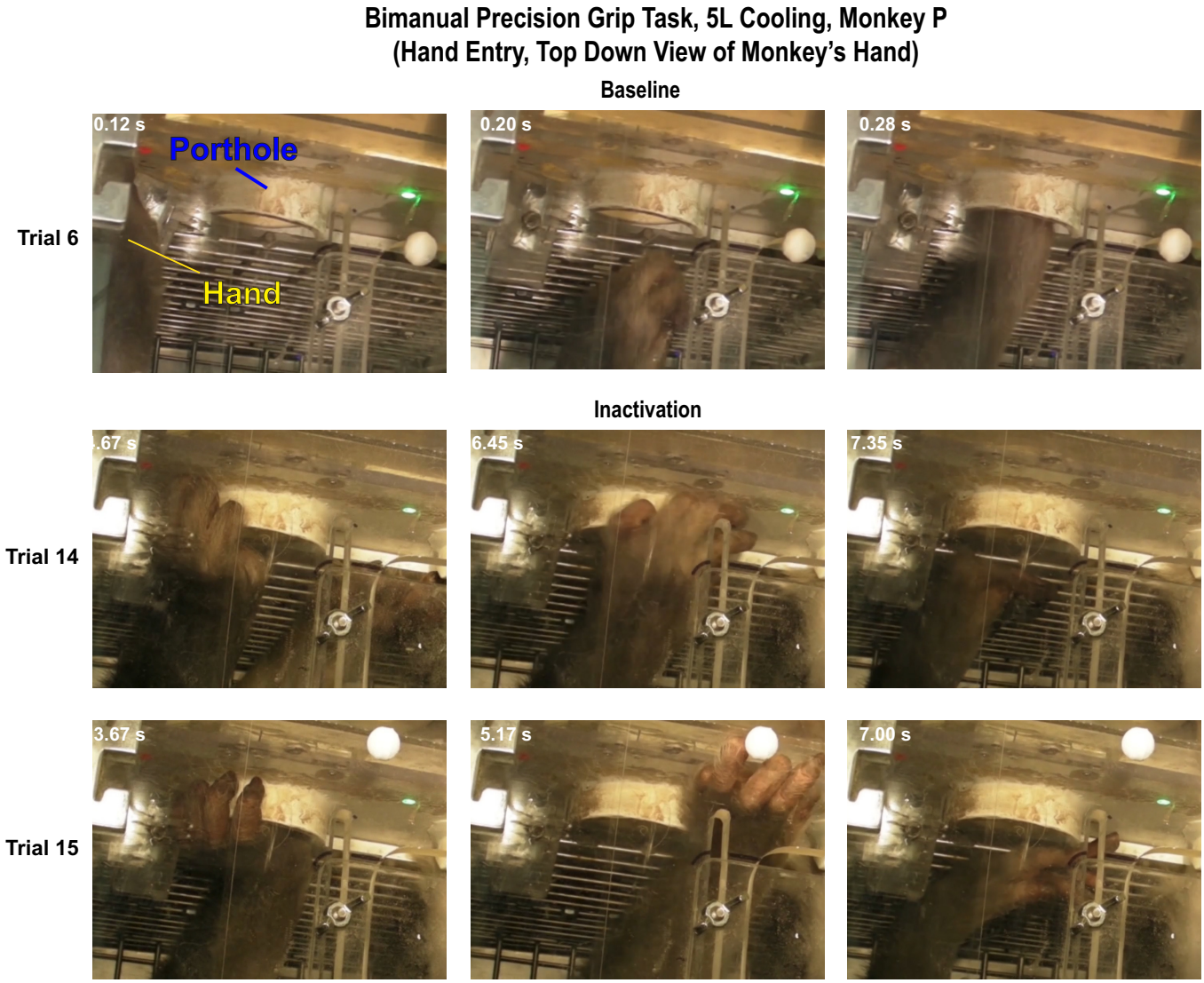

Figure 13. Bimanual precision grip task (*monkey P*, area 5L cooling; hand entry): still frames captured from a top-down angle centered on the monkey's left hand (contralateral to the cooled region) behind the viewing window. The hand is labeled in yellow, and the porthole to the task workspace is labeled in blue. Otherwise, conventions as in Figs. 11 and 12. During the Baseline epoch (*top*), the monkey quickly and easily reached its hand through the porthole and into the task workspace. During the Inactivation epoch (*bottom*, 2 trials shown) the monkey's starting position was often skewed, and its hand often collided with the edge of the porthole, the viewing window, or the inside of its primate chair.

and curvature that rely on proprioception (83, 85). Later studies using muscimol-based inactivation of comparatively smaller regions of area 2 described effects on grasping behavior. Hikosaka and colleagues (82) examined the effects of inactivating the anterior portion of area 2 where neurons responded to stimulation of the digits. They found that regardless of whether visual feedback was provided, monkeys displayed disrupted finger coordination and unstable positioning of the digits while extracting food from a recessed well or a funnel. The funnel grasping deficits were characterized by a somewhat spayed hand posture with improper extensions of the digits, similar to what we observed for both monkeys. In the same study in which they examined M1 inactivation, Brochier and colleagues (87) found that injections of muscimol in the antero-lateral portion of somatosensory cortex, which likely included area 2 but may also have included adjacent somatosensory fields, yielded abnormal grip postures, uncoordinated finger movements, and difficulty lifting objects despite observing no reduction in grip force. They also observed a disruption of precision grip behaviors during retrieval of a food item from a recessed well that was partially ameliorated when visual feedback was provided. Our results largely align with these previous studies in suggesting a role for area 2 in proprioceptive feedback that is most useful when visual feedback of a reach trajectory is removed. Although neither study described the hypometric reaches we observed, it is possible that inclusion of the forelimb representation in the inactivated region is responsible for this specific deficit. Importantly, our study is one of the few studies to examine the effects of inactivating a discrete portion of area 2 without encroaching on an adjacent cortical area (in the case of *monkey A*) and the first to employ a technique with a higher temporal resolution compared with chemical agents such as muscimol.

Area 7b

Although several studies have examined the manual deficits that occur with lesioning or deactivating the inferior parietal lobule (IPL), a large swath of cortex that includes a number of cortical fields, this is the first investigation that examines the behavioral deficits that occur after deactivation of area 7b specifically. Contemporary architectonic investigations of the IPL have subdivided area 7b into two distinct zones, PF and PFG (13, 31). Although our histological reconstruction did not differentiate between the two subdivisions of 7b, the placement of our cooling devices relative to 7b's overall architectonic borders and the intraparietal and lateral sulci indicate that for *monkey A* the cooling device was likely confined to the lateral portion of PF whereas for *monkey M* the cryoloop was in the rostro-medial portions of PF but also encroached on PFG (Fig. 4, *B* and *C*). Neurons in PF are driven by actions related to hand-mouth coordination, but they are predominantly tuned to facial movements and biting rather than arm or hand movements (8, 32). With regard to sensory responses, PF primarily contains neurons responsive to somatosensory stimulation of the orofacial region and contains very few responding to any visual stimuli (8). PFG has the largest mix of neurons tuned to different sensory modalities and motor actions (8). The somatosensory receptive fields of these neurons tend to be located on the hand and arm, whereas the neurons that respond to visual stimuli are primarily driven by objects placed within the monkey's reaching distance or exhibit "mirror neuron"-like responses. Neurons here respond to hand grasping and hand-mouth coordination during feeding. In addition, PFG contains neurons selective for action context that goes beyond the simple kinematics of the movement performed, i.e., the "why" of an action in addition to the "how" (88). Early lesion experiments of the IPL, which included portions of area 7b, noted that animals had a hesitance in using the contralateral limb and general impairments of grasping, especially when visual feedback was removed, as well as both hypometric and hypermetric reaches (113, 114). In situations where the unaffected arm was restrained, large area 7 ablations resulted in a refusal to use the contralateral limb, hypermetric reaches that drifted medial to the target food item, and an open-handed grasping posture in which digits were not opposed to each other during target acquisition (115). Reversible inactivation of the IPL with large cooling plates (66, 67) resulted in a type of hemineglect that precluded acting upon the contralateral visual hemifield, even with the ipsilateral hand. Although more contemporary inactivation studies have focused on individual regions around the IPL, to our knowledge all have focused on those located in the IPS (48–52, 65), with the anterior intraparietal area (AIP) being the most salient in terms of studying manual behaviors. For example, Gallese et al. (116) demonstrated that muscimol-based inactivation of portions of AIP resulted in a deficit in hand preshaping behavior before interacting with objects such that the hand posture was mismatched to an object's shape. Although AIP is directly adjacent to PFG and PF, we consider it unlikely that this area was affected by cooling since the cryoloop in *monkey M* only directly abutted the IPS at its rostral-most tip (Fig. 4). Taken together, our results support electrophysiological investigations suggesting a role for 7b in mid- to late-stage reaching and grasping behavior: inactivation seems to disrupt hand-mouth coordination in addition to grip aperture. It should be noted, however, that given the relatively rostro-medial location of the cryoloop placement in *monkey M*, it seems likely that we preferentially inactivated the rostro-medial portions of area PF and possibly a small portion of PFG, thus skewing our results toward deficits related to hand-mouth coordination rather than those related to reaches. This is important to consider when comparing these results to those we obtained when inactivating area 5L, an area containing somatosensory neurons that are exclusively tuned to stimulation of the arm and hand (e.g., Ref. 7). Although the deficits we observed do not exactly match those observed in previous loss-of-function studies, this is not surprising since we targeted a specific cortical field rather than lesioning/deactivating multiple cortical fields on the IPL. This highlights a major contribution of our results: inactivation of a discrete portion of the IPL comprised of subfields that seem to be responsible for contextually appropriate mid- to late-stage reaching and grasping behavior as well as hand-mouth coordination. Future work examining the contribution of the individual subfields (e.g., PFG and PG) will help elucidate whether their distinct electrophysiological profiles are reflected in functional contributions to reaching and grasping behavior.

Area 5L

Although there have been many studies examining the functional properties of medial and posterior regions on the superior parietal lobule (SPL; e.g., PEc, 5d, and PRR) and medial portions of the rostral bank of the intraparietal sulcus (e.g., MIP), comparatively fewer have recorded more laterally in the region that we designate as 5L (7). Among those few studies that have been conducted in awake, behaving monkeys, several have found that a large proportion of neurons are active before contacting an object (17, 74), with activity peaking just before contact (21, 22) and responses modulated by object shape (72) and object approach trajectory (23). In an earlier investigation, our laboratory examined the effects of small, restricted lesions targeting area 5L (35) on tasks very similar to those used here. Although those lesions caused a dramatic drop in the use of the contralesional hand and eventually a reduced success rate, the deficits were fleeting and overlapped the initial surgical recovery period, making it difficult to ascribe a specific role for 5L in manual behaviors. Previously, Stein (66, 67) cooled the entire gyral aspect of area 5, causing deficits in tactile discrimination and a general clumsiness in the contralateral limb even with visual guidance (and in both visual hemifields). More recently, muscimol has been employed to inactivate the "parietal reach region" (PRR; Refs. 42–47), whereas both muscimol and cryoloops have been used to inactivate portions of area 5 on the gyral surface of the SPL (40, 68). Although the studies of PRR inactivation demonstrated that inactivation impairs contralateral reaches or joystick movements (but not saccades), inactivating the caudomedial aspect of area 5 on the gyral surface produced deficits in both the trajectory and speed of corrective movements made to queued locations in three-dimensional space (40). In contrast, inactivating a more rostrolateral portion of area 5 on the gyral surface via cooling showed that

inactivation reduced spatial accuracy (but not the speed of corrective responses) in a postural perturbation task (68). Although these previous studies provided important insights into the role of particular posterior parietal areas in reaching and grasping, neither of those studies examined naturalistic reaching, grasping, and object manipulation behavior, nor did they examine any region overlapping area 5L. Although previous electrophysiological studies align with our results positing a role for area 5L in early- to mid-stage reaching and grasping behavior, the lack of comparable loss-of-function investigations highlights the importance of this study: This is the first investigation to examine the effects of reversible inactivation of area 5L (which is considered to be a distinct region within Brodmann's area 5, see Ref. 7). These results allowed us to assess the role of this region in reaching/grasping behavior without the rapid reorganization and behavioral recovery that make interpreting permanent lesions so difficult (35). That said, because of surgical constraints we were only able to collect area 5L deactivation data from one monkey (*monkey P*, see METHODS) using a task that the other two monkeys did not perform. As such, the conclusions we can draw from this aspect of the experiments are somewhat limited.

Laterality of Deficits and Bimanual Coordination

In all cases the deficits we observed were confined to the contralateral arm/hand. Given the prevalence of bilateral activation of motor and posterior parietal cortex in humans during reaching/grasping tasks (see Refs. 117, 118 for review), this may be a surprising result. Indeed, although the majority of neurons in macaque motor and parietal cortex respond to contralateral simulation of the body (or movements of the body), there are some studies that report bilateral receptive fields for neurons in some areas of parietal cortex (7, 8, 107, 119, 120) and some studies that have found neurons responsive to bilateral or ipsilateral movements in some regions of motor cortex (75, 121–125). Despite this, neither lesions nor reversible inactivation of these regions has been consistently shown to elicit bimanual or ipsilateral deficits (35, 44, 101, 115, 126, 127). Recent work by Mooshagian et al. (128, 129) recording both single-unit spiking activity as well as local field potentials from PRR in macaque monkeys has shed some light on this issue: ipsilateral responses in PRR neurons are likely driven either by stimuli in the neuron's visual receptive field or via interhemispheric communication. The same group also found that bilateral inactivation of several regions comprising PRR produced deficits that did not differ in effect size compared with unilateral inactivation, supporting the idea that PRR's functional contribution to reach planning is contralateral (47). Thus, it may be the case that although ipsilateral responses are observed in some regions within the fronto-parietal reaching and grasping network, these may only have functional consequences during bimanual coordination (if at all). Although the bimanual precision grip task described here does require the successful coordination of both hands to execute the task successfully, the task design makes it difficult to distinguish between a contralateral deficit and a deficit of bimanual coordination. Future work examining the function of these regions would greatly benefit from tasks that can disentangle these effects.

Caveats and Conclusions

Our goal was to understand the contribution of different regions of the fronto-parietal reaching and grasping network to ethologically relevant tasks. The heterogeneous and somewhat overlapping nature of the deficits that we observed can make ascribing a specific role to a given region difficult for two reasons. First, it is unlikely that there is a one-to-one correspondence between a particular cortical field and some aspect of behavior. Thus, part of the overlap in functions that we see following deactivation of different cortical fields is likely due to the distributed nature of these networks and a genuine overlap in the function between regions. Second, it is also possible that removing one node from this network could drive compensatory plasticity in the remaining nodes. This is supported by previous work in our own laboratory that demonstrates that deactivating portions of this network (M1, 5L, and 7b) immediately alters response properties and receptive field size and configuration of neurons in areas 1 and 2 (69, 70). In the present study, although many of the deficits we observed were quite profound during the first few sessions of cooling, often they would abate in subsequent sessions or even within the same session. Although it is possible that the across-session diminution of effects was due to thermal insulation of the cortex by granulation tissue (see RESULTS), this cannot explain the within-session effects. Whether this plasticity is driven by top-down changes in strategy (as suggested above) or bottom-up plasticity is a topic ripe for future investigations that examine combinatorial inactivation/electrophysiology both within and outside the fronto-parietal reaching and grasping network.

SUPPLEMENTAL DATA

Supplemental Videos S1–S5 and Supplemental Figs. S1–S5: https://doi.org/10.6084/m9.figshare.14802675.

ACKNOWLEDGMENTS

We thank Tingrui Pan, Arnold Chen, and Scott Simon for cooling chip development/construction); Adam Gordon, Conor Weatherford, and Raisa Rahim for running monkeys/data analysis; and Cynthia Weller and Mary Baldwin for brain cutting/histology.

GRANTS

This work was supported by National Institute of Neurological Disorders and Stroke Grant 5R01NS035103 (L. A. Krubitzer).

DISCLOSURES

No conflicts of interest, financial or otherwise, are declared by the authors.

AUTHOR CONTRIBUTIONS

A.B.G., D.F.C., G.H.R., and L.A.K. conceived and designed research; A.B.G., D.F.C., and C.R.P. performed experiments; A.B.G. and C.R.P. analyzed data; A.B.G., D.F.C., G.H.R., and L.A.K. interpreted results of experiments; A.B.G., D.F.C., and L.A.K. prepared figures; A.B.G. and L.A.K. drafted manuscript; A.B.G., D.F.C., G.H.R., and L.A.K. edited and revised manuscript; A.B.G., D.F.C., C.R.P., G.H.R., and L.A.K. approved final version of manuscript.

REFERENCES

1. **Andersen RA**, **Cui H.** Intention, action planning, and decision making in parietal-frontal circuits. *Neuron* 63: 568–583, 2009. doi:10.1016/j.neuron.2009.08.028.
2. **Gottlieb J**, **Snyder LH.** Spatial and non-spatial functions of the parietal cortex. *Curr Opin Neurobiol* 20: 731–740, 2010. doi:10.1016/j.conb.2010.09.015.
3. **Hadjidimitrakis K**, **Bakola S**, **Wong YT**, **Hagan MA.** Mixed spatial and movement representations in the primate posterior parietal cortex. *Front Neural Circuits* 13: 15, 2019. doi:10.3389/fncir.2019.00015.
4. **Caminiti R**, **Borra E**, **Visco-Comandini F**, **Battaglia-Mayer A**, **Averbeck BB**, **Luppino G.** Computational architecture of the parieto-frontal network underlying cognitive-motor control in monkeys. *eNeuro* 4: ENEURO.0306-16.2017, 2017. doi:10.1523/ENEURO.0306-16.2017.
5. **Cooke DF**, **Goldring A**, **Recanzone GH**, **Krubitzer L.** The evolution of parietal areas associated with visuomanual behavior: from grasping to tool use. In: *The Visual Neurosciences*, edited by Chalupa L, Werner J. Cambridge, MA: MIT Press, 2013, p**.** 1049–1063.
6. **Goldring AB**, **Krubitzer LA.** Evolution of parietal cortex in mammals: from manipulation to tool use. In: *The Evolution of Nervous Systems* (2nd ed.), edited by Krubitzer L, Kaas JH. London: Elsevier, 2016, vol**.** 3, chapt. 14, p. 259–286.
7. **Seelke AM**, **Padberg JJ**, **Disbrow E**, **Purnell SM**, **Recanzone G**, **Krubitzer L.** Topographic maps within Brodmann's area 5 of macaque monkeys. *Cereb Cortex* 22: 1834–1850, 2012. doi:10.1093/cercor/bhr257.
8. **Rozzi S**, **Ferrari PF**, **Bonini L**, **Rizzolatti G**, **Fogassi L.** Functional organization of inferior parietal lobule convexity in the macaque monkey: electrophysiological characterization of motor, sensory and mirror responses and their correlation with cytoarchitectonic areas. *Eur J Neurosci* 28: 1569–1588, 2008. doi:10.1111/j.1460-9568.2008.06395.x.
9. **Klam F**, **Graf W.** Discrimination between active and passive head movements by macaque ventral and medial intraparietal cortex neurons. *J Physiol* 574: 367–386, 2006. doi:10.1113/jphysiol.2005.103697.
10. **Bakola S**, **Passarelli L**, **Huynh T**, **Impieri D**, **Worthy KH**, **Fattori P**, **Galletti C**, **Burman KJ**, **Rosa MG.** Cortical afferents and myeloarchitecture distinguish the medial intraparietal area (MIP) from neighboring subdivisions of the macaque cortex. *eNeuro* 4: ENEURO.0344-17.2017, 2017. doi:10.1523/ENEURO.0344-17.2017.
11. **Borra E**, **Luppino G.** Functional anatomy of the macaque temporo-parieto-frontal connectivity. *Cortex* 97: 306–326, 2017. doi:10.1016/j.cortex.2016.12.007.
12. **Caminiti R**, **Girard G**, **Battaglia-Mayer A**, **Borra E**, **Schito A**, **Innocenti GM**, **Luppino G.** The complex hodological architecture of the macaque dorsal intraparietal areas as emerging from neural tracers and dw-mri tractography. *eNeuro* 8: ENEURO.0102-21.2021, 2021. doi:10.1523/ENEURO.0102-21.2021.
13. **Pandya D**, **Seltzer B.** Intrinsic connections and architectonics of posterior parietal cortex in the rhesus monkey. *J Comp Neurol* 204: 196–210, 1982. doi:10.1002/cne.902040208.
14. **Seltzer B**, **Pandya D.** Posterior parietal projections to the intraparietal sulcus of the rhesus monkey. *Exp Brain Res* 62: 459–469, 1986. doi:10.1007/BF00236024.
15. **Lewis JW**, **Van Essen DC.** Mapping of architectonic subdivisions in the macaque monkey, with emphasis on parieto-occipital cortex. *J Comp Neurol* 428: 79–111, 2000. doi:10.1002/1096-9861(20001204)428:1<79::AID-CNE7>3.0.CO;2-Q.
16. **Snyder LH**, **Batista AP**, **Andersen RA.** Coding of intention in the posterior parietal cortex. *Nature* 386: 167–170, 1997. doi:10.1038/386167a0.
17. **Debowy DJ**, **Ghosh S**, **Ro JY**, **Gardner EP.** Comparison of neuronal firing rates in somatosensory and posterior parietal cortex during prehension. *Exp Brain Res* 137: 269–291, 2001. doi:10.1007/s002210000660.
18. **Calton JL**, **Dickinson AR**, **Snyder LH.** Non-spatial, motor-specific activation in posterior parietal cortex. *Nat Neurosci* 5: 580–588, 2002. doi:10.1038/nn0602-862.
19. **Kalaska JF.** Parietal cortex area 5 and visuomotor behavior. *Can J Physiol Pharmacol* 74: 483–498, 1996. doi:10.1139/y96-040.
20. **Wise SP**, **Boussaoud D**, **Johnson PB**, **Caminiti R.** Premotor and parietal cortex: corticocortical connectivity and combinatorial computations. *Annu Rev Neurosci* 20: 25–42, 1997. doi:10.1146/annurev.neuro.20.1.25.
21. **Gardner EP**, **Babu KS**, **Reitzen SD**, **Ghosh S**, **Brown AS**, **Chen J**, **Hall AL**, **Herzlinger MD**, **Kohlenstein JB**, **Ro JY.** Neurophysiology of prehension. I. Posterior parietal cortex and object-oriented hand behaviors. *J Neurophysiol* 97: 387–406, 2007. doi:10.1152/jn.00558.2006.
22. **Gardner EP**, **Ro JY**, **Babu KS**, **Ghosh S.** Neurophysiology of prehension. II. Response diversity in primary somatosensory (S-I) and motor (M-I) cortices. *J Neurophysiol* 97: 1656–1670, 2007. doi:10.1152/jn.01031.2006.
23. **Chen J**, **Reitzen SD**, **Kohlenstein JB**, **Gardner EP.** Neural representation of hand kinematics during prehension in posterior parietal cortex of the macaque monkey. *J Neurophysiol* 102: 3310–3328, 2009. doi:10.1152/jn.90942.2008.
24. **Ferraina S**, **Bianchi L.** Posterior parietal cortex: functional properties of neurons in area 5 during an instructed-delay reaching task within different parts of space. *Exp Brain Res* 99: 175–178, 1994. doi:10.1007/BF00241423.
25. **Lacquaniti F**, **Guigon E**, **Bianchi L**, **Ferraina S**, **Caminiti R.** Representing spatial information for limb movement: role of area 5 in the monkey. *Cereb Cortex* 5: 391–409, 1995. doi:10.1093/cercor/5.5.391.
26. **Cohen YE**, **Andersen RA.** Reaches to sounds encoded in an eye-centered reference frame. *Neuron* 27: 647–652, 2000. doi:10.1016/S0896-6273(00)00073-8.
27. **Padberg J**, **Cooke DF**, **Cerkevich CM**, **Kaas JH**, **Krubitzer L.** Cortical connections of area 2 and posterior parietal area 5 in macaque monkeys. *J Comp Neurol* 527: 718–737, 2019. doi:10.1002/cne.24453.
28. **Seltzer B**, **Pandya D.** Converging visual and somatic sensory cortical input to the intraparietal sulcus of the rhesus monkey. *Brain Res* 192: 339–351, 1980. doi:10.1016/0006-8993(80)90888-4.
29. **Preuss TM**, **Goldman-Rakic PS.** Architectonics of the parietal and temporal association cortex in the strepsirhine primate *Galago* compared to the anthropoid primate *Macaca*. *J Comp Neurol* 310: 475–506, 1991. doi:10.1002/cne.903100403.
30. **Lewis JW**, **Van Essen DC.** Corticocortical connections of visual, sensorimotor, and multimodal processing areas in the parietal lobe of the macaque monkey. *J Comp Neurol* 428: 112–137, 2000. doi:10.1002/1096-9861(20001204)428:1<112::AID-CNE8>3.0.CO;2-9.
31. **Gregoriou GG**, **Borra E**, **Matelli M**, **Luppino G.** Architectonic organization of the inferior parietal convexity of the macaque monkey. *J Comp Neurol* 496: 422–451, 2006. doi:10.1002/cne.20933.
32. **Yokochi H**, **Tanaka M**, **Kumashiro M**, **Iriki A.** Inferior parietal somatosensory neurons coding face-hand coordination in Japanese macaques. *Somatosens Mot Res* 20: 115–125, 2003. doi:10.1080/0899022031000105145.
33. **Fogassi L**, **Ferrari PF**, **Gesierich B**, **Rozzi S**, **Chersi F**, **Rizzolatti G.** Parietal lobe: from action organization to intention understanding. *Science* 308: 662–667, 2005. doi:10.1126/science.1106138.
34. **Bonini L**, **Serventi FU**, **Simone L**, **Rozzi S**, **Ferrari PF**, **Fogassi L.** Grasping neurons of monkey parietal and premotor cortices encode action goals at distinct levels of abstraction during complex action sequences. *J Neurosci* 31: 5876–5886, 2011. doi:10.1523/JNEUROSCI.5186-10.2011.
35. **Padberg J**, **Recanzone G**, **Engle J**, **Cooke D**, **Goldring A**, **Krubitzer L.** Lesions in posterior parietal area 5 in monkeys result in rapid behavioral and cortical plasticity. *J Neurosci* 30: 12918–12935, 2010. doi:10.1523/JNEUROSCI.1806-10.2010.
36. **Rushworth MF**, **Nixon PD**, **Passingham RE.** Parietal cortex and movement. I. Movement selection and reaching. *Exp Brain Res* 117: 292–310, 1997. doi:10.1007/s002210050224.
37. **Rushworth MF**, **Nixon PD**, **Passingham RE.** Parietal cortex and movement. II. Spatial representation. *Exp Brain Res* 117: 311–323, 1997. doi:10.1007/s002210050225.
38. **Rushworth MF**, **Johansen-Berg H**, **Young SA.** Parietal cortex and spatial-postural transformation during arm movements. *J Neurophysiol* 79: 478–482, 1998. doi:10.1152/jn.1998.79.1.478.
39. **Lamotte RH**, **Acuña C.** Defects in accuracy of reaching after removal of posterior parietal cortex in monkeys. *Brain Res* 139: 309–326, 1978. doi:10.1016/0006-8993(78)90931-9.

40. **Battaglia-Mayer A**, **Ferrari-Toniolo S**, **Visco-Comandini F**, **Archambault PS**, **Saberi-Moghadam S**, **Caminiti R.** Impairment of online control of hand and eye movements in a monkey model of optic ataxia. *Cereb Cortex* 23: 2644–2656, 2013. doi:10.1093/cercor/bhs250.
41. **Sawamura H**, **Shima K**, **Tanji J.** Deficits in action selection based on numerical information after inactivation of the posterior parietal cortex in monkeys. *J Neurophysiol* 104: 902–910, 2010. doi:10.1152/jn.01014.2009.
42. **Hwang EJ**, **Hauschild M**, **Wilke M**, **Andersen RA.** Inactivation of the parietal reach region causes optic ataxia, impairing reaches but not saccades. *Neuron* 76: 1021–1029, 2012. doi:10.1016/j.neuron.2012.10.030.
43. **Hwang EJ**, **Hauschild M**, **Wilke M**, **Andersen RA.** Spatial and temporal eye-hand coordination relies on the parietal reach region. *J Neurosci* 34: 12884–12892, 2014. doi:10.1523/JNEUROSCI.3719-13.2014.
44. **Yttri EA**, **Wang C**, **Liu Y**, **Snyder LH.** The parietal reach region is limb specific and not involved in eye-hand coordination. *J Neurophysiol* 111: 520–532, 2014. doi:10.1152/jn.00058.2013.
45. **Christopoulos VN**, **Bonaiuto J**, **Kagan I**, **Andersen RA.** Inactivation of parietal reach region affects reaching but not saccade choices in internally guided decisions. *J Neurosci* 35: 11719–11728, 2015. doi:10.1523/JNEUROSCI.1068-15.2015.
46. **Kubanek J**, **Li JM**, **Snyder LH.** Motor role of parietal cortex in a monkey model of hemispatial neglect. *Proc Natl Acad Sci USA* 112: E2067–E2072, 2015. doi:10.1073/pnas.1418324112.
47. **Mooshagian E**, **Yttri EA**, **Loewy AD**, **Snyder LH.** Contralateral limb specificity for movement preparation in the parietal reach region. *J Neurosci* 42: 1692–1701, 2022. doi:10.1523/JNEUROSCI.0232-21.2021.
48. **Van Dromme IC**, **Premereur E**, **Verhoef BE**, **Vanduffel W**, **Janssen P.** Posterior parietal cortex drives inferotemporal activations during three-dimensional object vision. *PLoS Biol* 14: e1002445, 2016. doi:10.1371/journal.pbio.1002445.
49. **Li CS**, **Mazzoni P**, **Andersen RA.** Effect of reversible inactivation of macaque lateral intraparietal area on visual and memory saccades. *J Neurophysiol* 81: 1827–1838, 1999. doi:10.1152/jn.1999.81.4.1827.
50. **Katz LN**, **Yates JL**, **Pillow JW**, **Huk AC.** Dissociated functional significance of choice-related activity across the primate dorsal stream. *Nature* 535: 285–288, 2016. doi:10.1038/nature18617.
51. **Zhou Y**, **Freedman DJ.** Posterior parietal cortex plays a causal role in perceptual and categorical decisions. *Science* 365: 180–185, 2019. doi:10.1126/science.aaw8347.
52. **DeWind NK**, **Peng J**, **Luo A**, **Brannon EM**, **Platt ML.** Pharmacological inactivation does not support a unique causal role for intraparietal sulcus in the discrimination of visual number. *PLoS One* 12: e0188820, 2017. doi:10.1371/journal.pone.0188820.
53. **Malpeli JG.** Reversible inactivation of subcortical sites by drug injection. *J Neurosci Methods* 86: 119–128, 1999. doi:10.1016/S0165-0270(98)00161-7.
54. **Lomber SG.** The advantages and limitations of permanent or reversible deactivation techniques in the assessment of neural function. *J Neurosci Methods* 86: 109–117, 1999. doi:10.1016/S0165-0270(98)00160-5.
55. **Dai J**, **Brooks DI**, **Sheinberg DL.** Optogenetic and electrical microstimulation systematically bias visuospatial choice in primates. *Curr Biol* 24: 63–69, 2014. doi:10.1016/j.cub.2013.11.011.
56. **Lomber SG**, **Payne BR**, **Horel JA.** The cryoloop: an adaptable reversible cooling deactivation method for behavioral or electrophysiological assessment of neural function. *J Neurosci Methods* 86: 179–194, 1999. doi:10.1016/s0165-0270(98)00165-4.
57. **Ponce CR**, **Lomber SG**, **Born RT.** Integrating motion and depth via parallel pathways. *Nat Neurosci* 11: 216–223, 2008. doi:10.1038/nn2039.
58. **Ponce CR**, **Hunter JN**, **Pack CC**, **Lomber SG**, **Born RT.** Contributions of indirect pathways to visual response properties in macaque middle temporal area MT. *J Neurosci* 31: 3894–3903, 2011. doi:10.1523/JNEUROSCI.5362-10.2011.
59. **Peel TR**, **Dash S**, **Lomber SG**, **Corneil BD.** Frontal eye field inactivation diminishes superior colliculus activity, but delayed saccadic accumulation governs reaction time increases. *J Neurosci* 37: 11715–11730, 2017. doi:10.1523/JNEUROSCI.2664-17.2017.
60. **Nassi JJ**, **Lomber SG**, **Born RT.** Corticocortical feedback contributes to surround suppression in V1 of the alert primate. *J Neurosci* 33: 8504–8517, 2013. doi:10.1523/JNEUROSCI.5124-12.2013.
61. **Koval MJ**, **Lomber SG**, **Everling S.** Prefrontal cortex deactivation in macaques alters activity in the superior colliculus and impairs voluntary control of saccades. *J Neurosci* 31: 8659–8668, 2011. doi:10.1523/JNEUROSCI.1258-11.2011.
62. **Johnston K**, **Lomber SG**, **Everling S.** Unilateral deactivation of macaque dorsolateral prefrontal cortex induces biases in stimulus selection. *J Neurophysiol* 115: 1468–1476, 2016. doi:10.1152/jn.00563.2015.
63. **Ma L**, **Chan JL**, **Johnston K**, **Lomber SG**, **Everling S.** Macaque anterior cingulate cortex deactivation impairs performance and alters lateral prefrontal oscillatory activities in a rule-switching task. *PLoS Biol* 17: e3000045, 2019. doi:10.1371/journal.pbio.3000045.
64. **Plakke B**, **Hwang J**, **Romanski LM.** Inactivation of primate prefrontal cortex impairs auditory and audiovisual working memory. *J Neurosci* 35: 9666–9675, 2015. doi:10.1523/JNEUROSCI.1218-15.2015.
65. **Chen X**, **Zirnsak M**, **Vega GM**, **Govil E**, **Lomber SG**, **Moore T.** Parietal cortex regulates visual salience and salience-driven behavior. *Neuron* 106: 177–187.e4, 2020. doi:10.1016/j.neuron.2020.01.016.
66. **Stein J.** Proceedings: the effect of cooling parietal lobe areas 5 and 7 upon voluntary movement in awake rhesus monkeys. *J Physiol* 258: 62P–63P, 1976.
67. **Stein J.** Effects of parietal lobe cooling on manipulative behaviour in the conscious monkey. In: *Active Touch. The Mechanisms of Recognition of Objects by Manipulation: A Multidisciplinary Approach*, edited by Gordon G. Oxford, UK: Pergamon, 1978, p. 79–90.
68. **Takei T**, **Lomber SG**, **Cook DJ**, **Scott SH.** Transient deactivation of dorsal premotor cortex or parietal area 5 impairs feedback control of the limb in macaques. *Curr Biol* 31: 1476–1487.e5, 2021. doi:10.1016/j.cub.2021.01.049.
69. **Cooke DF**, **Goldring AB**, **Baldwin MK**, **Recanzone GH**, **Chen A**, **Pan T**, **Simon SI**, **Krubitzer L.** Reversible deactivation of higher-order posterior parietal areas. I. Alterations of receptive field characteristics in early stages of neocortical processing. *J Neurophysiol* 112: 2529–2544, 2014. doi:10.1152/jn.00140.2014.
70. **Goldring AB**, **Cooke DF**, **Baldwin MK**, **Recanzone GH**, **Gordon AG**, **Pan T**, **Simon SI**, **Krubitzer L.** Reversible deactivation of higher-order posterior parietal areas. II. Alterations in response properties of neurons in areas 1 and 2. *J Neurophysiol* 112: 2545–2560, 2014. doi:10.1152/jn.00141.2014.
71. **Cooke DF**, **Goldring AB**, **Yamayoshi I**, **Tsourkas P**, **Recanzone GH**, **Tiriac A**, **Pan T**, **Simon SI**, **Krubitzer L.** Fabrication of an inexpensive, implantable cooling device for reversible brain deactivation in animals ranging from rodents to primates. *J Neurophysiol* 107: 3543–3558, 2012. doi:10.1152/jn.01101.2011.
72. **Gardner EP**, **Babu KS**, **Ghosh S**, **Sherwood A**, **Chen J.** Neurophysiology of prehension. III. Representation of object features in posterior parietal cortex of the macaque monkey. *J Neurophysiol* 98: 3708–3730, 2007. doi:10.1152/jn.00609.2007.
73. **Salimi I**, **Brochier T**, **Smith AM.** Neuronal activity in somatosensory cortex of monkeys using a precision grip. I. Receptive fields and discharge patterns. *J Neurophysiol* 81: 825–834, 1999. doi:10.1152/jn.1999.81.2.825.
74. **Gardner EP**, **Ro JY**, **Debowy D**, **Ghosh S.** Facilitation of neuronal activity in somatosensory and posterior parietal cortex during prehension. *Exp Brain Res* 127: 329–354, 1999. doi:10.1007/s002210050803.
75. **Cisek P**, **Crammond DJ**, **Kalaska JF.** Neural activity in primary motor and dorsal premotor cortex in reaching tasks with the contralateral versus ipsilateral arm. *J Neurophysiol* 89: 922–942, 2003. doi:10.1152/jn.00607.2002.
76. **Fu QG**, **Suarez JI**, **Ebner TJ.** Neuronal specification of direction and distance during reaching movements in the superior precentral premotor area and primary motor cortex of monkeys. *J Neurophysiol* 70: 2097–2116, 1993. doi:10.1152/jn.1993.70.5.2097.
77. **Caminiti R**, **Johnson PB**, **Urbano A.** Making arm movements within different parts of space: dynamic aspects in the primate motor cortex. *J Neurosci* 10: 2039–2058, 1990. doi:10.1523/JNEUROSCI.10-07-02039.1990.
78. **Schaffelhofer S**, **Agudelo-Toro A**, **Scherberger H.** Decoding a wide range of hand configurations from macaque motor, premotor, and

parietal cortices. *J Neurosci* 35: 1068–1081, 2015. doi:10.1523/JNEUROSCI.3594-14.2015.
79. **Archambault PS**, **Ferrari-Toniolo S**, **Battaglia-Mayer A.** Online control of hand trajectory and evolution of motor intention in the parietofrontal system. *J Neurosci* 31: 742–752, 2011. doi:10.1523/JNEUROSCI.2623-10.2011.
80. **Gardner E.** Somatosensory cortical mechanisms of feature detection in tactile and kinesthetic discrimination. *Can J Physiol Pharmacol* 66: 439–454, 1988. doi:10.1139/y88-074.
81. **Yau JM**, **Connor CE**, **Hsiao SS.** Representation of tactile curvature in macaque somatosensory area 2. *J Neurophysiol* 109: 2999–3012, 2013. doi:10.1152/jn.00804.2012.
82. **Hikosaka O**, **Tanaka M**, **Sakamoto M**, **Iwamura Y.** Deficits in manipulative behaviors induced by local injections of muscimol in the first somatosensory cortex of the conscious monkey. *Brain Res* 325: 375–380, 1985. doi:10.1016/0006-8993(85)90344-0.
83. **Randolph M**, **Semmes J.** Behavioral consequences of selective subtotal ablations in the postcentral gyrus of *Macaca mulatta*. *Brain Res* 70: 55–70, 1974. doi:10.1016/0006-8993(74)90211-X.
84. **Semmes J**, **Turner B.** Effects of cortical lesions on somatosensory tasks. *J Invest Dermatol* 69: 181–189, 1977. doi:10.1111/1523-1747.ep12497948.
85. **Carlson M.** Characteristics of sensory deficits following lesions of Brodmann's areas 1 and 2 in the postcentral gyrus of *Macaca mulatta*. *Brain Res* 204: 424–430, 1981. doi:10.1016/0006-8993(81)90602-8.
86. **London BM**, **Miller LE.** Responses of somatosensory area 2 neurons to actively and passively generated limb movements. *J Neurophysiol* 109: 1505–1513, 2013. doi:10.1152/jn.00372.2012.
87. **Brochier T**, **Boudreau MJ**, **Paré M**, **Smith AM.** The effects of muscimol inactivation of small regions of motor and somatosensory cortex on independent finger movements and force control in the precision grip. *Exp Brain Res* 128: 31–40, 1999. doi:10.1007/s002210050814.
88. **Bonini L**, **Ugolotti Serventi F**, **Bruni S**, **Maranesi M**, **Bimbi M**, **Simone L**, **Rozzi S**, **Ferrari PF**, **Fogassi L.** Selectivity for grip type and action goal in macaque inferior parietal and ventral premotor grasping neurons. *J Neurophysiol* 108: 1607–1619, 2012. doi:10.1152/jn.01158.2011.
89. **Overton JA**, **Cooke DF**, **Goldring AB**, **Lucero SA**, **Weatherford C**, **Recanzone GH.** Improved methods for acrylic-free implants in nonhuman primates for neuroscience research. *J Neurophysiol* 118: 3252–3270, 2017. doi:10.1152/jn.00191.2017.
90. **Antunes FM**, **Malmierca MS.** Effect of auditory cortex deactivation on stimulus-specific adaptation in the medial geniculate body. *J Neurosci* 31: 17306–17316, 2011. doi:10.1523/JNEUROSCI.1915-11.2011.
91. **Coomber B**, **Edwards D**, **Jones SJ**, **Shackleton TM**, **Goldschmidt J**, **Wallace MN**, **Palmer AR.** Cortical inactivation by cooling in small animals. *Front Syst Neurosci* 5: 53, 2011. doi:10.3389/fnsys.2011.00053.
92. **Cooke DF**, **Stepniewska I**, **Miller DJ**, **Kaas JH**, **Krubitzer L.** Reversible deactivation of motor cortex reveals functional connectivity with posterior parietal cortex in the prosimian Galago (*Otolemur garnettii*). *J Neurosci* 35: 14406–14422, 2015. doi:10.1523/JNEUROSCI.1468-15.2015.
93. **Gallyas F.** Silver staining of myelin by means of physical development. *Neurol Res* 1: 203–209, 1979. doi:10.1080/01616412.1979.11739553.
94. **Campbell MJ**, **Morrison JH.** Monoclonal antibody to neurofilament protein (SMI-32) labels a subpopulation of pyramidal neurons in the human and monkey neocortex. *J Comp Neurol* 282: 191–205, 1989. doi:10.1002/cne.902820204.
95. **Aihara H**, **Okada Y**, **Tamaki N.** The effects of cooling and rewarming on the neuronal activity of pyramidal neurons in guinea pig hippocampal slices. *Brain Res* 893: 36–45, 2001. doi:10.1016/s0006-8993(00)03285-6.
96. **Volgushev M**, **Kudryashov I**, **Chistiakova M**, **Mukovski M**, **Niesmann J**, **Eysel UT.** Probability of transmitter release at neocortical synapses at different temperatures. *J Neurophysiol* 92: 212–220, 2004. doi:10.1152/jn.01166.2003.
97. **Hoogewoud F**, **Hamadjida A**, **Wyss AF**, **Mir A**, **Schwab ME**, **Belhaj-Saif A**, **Rouiller EM.** Comparison of functional recovery of manual dexterity after unilateral spinal cord lesion or motor cortex lesion in adult macaque monkeys. *Front Neurol* 4: 101, 2013. doi:10.3389/fneur.2013.00101.
98. **Savidan J**, **Kaeser M**, **Belhaj-Saïf A**, **Schmidlin E**, **Rouiller EM.** Role of primary motor cortex in the control of manual dexterity assessed via sequential bilateral lesion in the adult macaque monkey: a case study. *Neuroscience* 357: 303–324, 2017. doi:10.1016/j.neuroscience.2017.06.018.
99. **Baldwin MK**, **Cooke DF**, **Goldring AB**, **Krubitzer L.** Representations of fine digit movements in posterior and anterior parietal cortex revealed using long-train intracortical microstimulation in macaque monkeys. *Cereb Cortex* 28: 4244–4263, 2018. doi:10.1093/cercor/bhx279.
100. **Matsumura M**, **Sawaguchi T**, **Oishi T**, **Ueki K**, **Kubota K.** Behavioral deficits induced by local injection of bicuculline and muscimol into the primate motor and premotor cortex. *J Neurophysiol* 65: 1542–1553, 1991. doi:10.1152/jn.1991.65.6.1542.
101. **Fogassi L**, **Gallese V**, **Buccino G**, **Craighero L**, **Fadiga L**, **Rizzolatti G.** Cortical mechanism for the visual guidance of hand grasping movements in the monkey: a reversible inactivation study. *Brain* 124: 571–586, 2001. doi:10.1093/brain/124.3.571.
102. **Cooke DF**, **Goldring AB**, **Baldwin MK**, **Donaldson MS**, **Krubitzer LA.** Reversible deactivation of motor cortex reveals functional connectivity with anterior and posterior parietal cortex in Old World monkeys (*Macaca mulatta*) (Abstract). *Soc Neurosci Abstr* 342: 14, 2015.
103. **He SQ**, **Dum RP**, **Strick PL.** Topographic organization of corticospinal projections from the frontal lobe: motor areas on the lateral surface of the hemisphere. *J Neurosci* 13: 952–980, 1993. doi:10.1523/JNEUROSCI.13-03-00952.1993.
104. **Dum RP**, **Strick PL.** The origin of corticospinal projections from the premotor areas in the frontal lobe. *J Neurosci* 11: 667–689, 1991. doi:10.1523/JNEUROSCI.11-03-00667.1991.
105. **Strick PL**, **Dum RP**, **Rathelot JA.** The cortical motor areas and the emergence of motor skills: a neuroanatomical perspective. *Annu Rev Neurosci* 44: 425–447, 2021. doi:10.1146/annurev-neuro-070918-050216.
106. **Rathelot JA**, **Strick PL.** Subdivisions of primary motor cortex based on cortico-motoneuronal cells. *Proc Natl Acad Sci USA* 106: 918–923, 2009. doi:10.1073/pnas.0808362106.
107. **Taoka M**, **Toda T**, **Iwamura Y.** Representation of the midline trunk, bilateral arms, and shoulders in the monkey postcentral somatosensory cortex. *Exp Brain Res* 123: 315–322, 1998. doi:10.1007/s002210050574.
108. **Iwamura Y**, **Tanaka M**, **Hikosaka O.** Overlapping representation of fingers in the somatosensory cortex (area 2) of the conscious monkey. *Brain Res* 197: 516–520, 1980. doi:10.1016/0006-8993(80)91139-7.
109. **Ageranioti-Bélanger S**, **Chapman C.** Discharge properties of neurones in the hand area of primary somatosensory cortex in monkeys in relation to the performance of an active tactile discrimination task. *Exp Brain Res* 91: 207–228, 1992. doi:10.1007/BF00231655.
110. **Pearson RC**, **Powell TP.** The projection of the primary somatic sensory cortex upon area 5 in the monkey. *Brain Res* 356: 89–107, 1985. doi:10.1016/0165-0173(85)90020-7.
111. **Pons TP**, **Kaas JH.** Corticocortical connections of area 2 of somatosensory cortex in macaque monkeys: a correlative anatomical and electrophysiological study. *J Comp Neurol* 248: 313–335, 1986. doi:10.1002/cne.902480303.
112. **Bakola S**, **Gamberini M**, **Passarelli L**, **Fattori P**, **Galletti C.** Cortical connections of parietal field PEc in the macaque: linking vision and somatic sensation for the control of limb action. *Cereb Cortex* 20: 2592–2604, 2010. doi:10.1093/cercor/bhq007.
113. **Peele T.** Acute and chronic parietal lobe ablations in monkeys. *J Nerv Ment Dis* 104: 340, 1946. doi:10.1097/00005053-194609000-00016.
114. **Fleming JF**, **Crosby EC.** The parietal lobe as an additional motor area; the motor effects of electrical stimulation and ablation of cortical areas 5 and 7 in monkeys. *J Comp Neurol* 103: 485–512, 1955. doi:10.1002/cne.901030306.
115. **Faugier-Grimaud S**, **Frenois C**, **Stein DG.** Effects of posterior parietal lesions on visually guided behavior in monkeys. *Neuropsychologia* 16: 151–168, 1978. doi:10.1016/0028-3932(78)90103-3.
116. **Gallese V**, **Murata A**, **Kaseda M**, **Niki N**, **Sakata H.** Deficit of hand preshaping after muscimol injection in monkey parietal cortex. *Neuroreport* 5: 1525–1529, 1994. doi:10.1097/00001756-199407000-00029.

117. **Vingerhoets G.** Contribution of the posterior parietal cortex in reaching, grasping, and using objects and tools. *Front Psychol* 5: 151, 2014. doi:10.3389/fpsyg.2014.00151.
118. **Bundy DT**, **Leuthardt EC.** The cortical physiology of ipsilateral limb movements. *Trends Neurosci* 42: 825–839, 2019. doi:10.1016/j.tins.2019.08.008.
119. **Iwamura Y**, **Iriki A**, **Tanaka M.** Bilateral hand representation in the postcentral somatosensory cortex. *Nature* 369: 554–556, 1994. doi:10.1038/369554a0.
120. **Iwamura Y**, **Tanaka M**, **Iriki A**, **Taoka M**, **Toda T.** Processing of tactile and kinesthetic signals from bilateral sides of the body in the postcentral gyrus of awake monkeys. *Behav Brain Res* 135: 185–190, 2002. doi:10.1016/s0166-4328(02)00164-x.
121. **Ganguly K**, **Secundo L**, **Ranade G**, **Orsborn A**, **Chang EF**, **Dimitrov DF**, **Wallis JD**, **Barbaro NM**, **Knight RT**, **Carmena JM.** Cortical representation of ipsilateral arm movements in monkey and man. *J Neurosci* 29: 12948–12956, 2009. doi:10.1523/JNEUROSCI.2471-09.2009.
122. **Donchin O**, **Gribova A**, **Steinberg O**, **Mitz AR**, **Bergman H**, **Vaadia E.** Single-unit activity related to bimanual arm movements in the primary and supplementary motor cortices. *J Neurophysiol* 88: 3498–3517, 2002. doi:10.1152/jn.00335.2001.
123. **Donchin O**, **Gribova A**, **Steinberg O**, **Bergman H**, **Vaadia E.** Primary motor cortex is involved in bimanual coordination. *Nature* 395: 274–278, 1998. doi:10.1038/26220.
124. **Matsunami K**, **Hamada I.** Characteristics of the ipsilateral movement-related neuron in the motor cortex of the monkey. *Brain Res* 204: 29–42, 1981. doi:10.1016/0006-8993(81)90649-1.
125. **Tanji J**, **Okano K**, **Sato KC.** Neuronal activity in cortical motor areas related to ipsilateral, contralateral, and bilateral digit movements of the monkey. *J Neurophysiol* 60: 325–343, 1988. doi:10.1152/jn.1988.60.1.325.
126. **Bashir S**, **Kaeser M**, **Wyss A**, **Hamadjida A**, **Liu Y**, **Bloch J**, **Brunet JF**, **Belhaj-Saif A**, **Rouiller EM.** Short-term effects of unilateral lesion of the primary motor cortex (M1) on ipsilesional hand dexterity in adult macaque monkeys. *Brain Struct Funct* 217: 63–79, 2012. doi:10.1007/s00429-011-0327-8.
127. **Kaeser M**, **Wyss AF**, **Bashir S**, **Hamadjida A**, **Liu Y**, **Bloch J**, **Brunet JF**, **Belhaj-Saif A**, **Rouiller EM.** Effects of unilateral motor cortex lesion on ipsilesional hand's reach and grasp performance in monkeys: relationship with recovery in the contralesional hand. *J Neurophysiol* 103: 1630–1645, 2010. doi:10.1152/jn.00459.2009.
128. **Mooshagian E**, **Wang C**, **Holmes CD**, **Snyder LH.** Single units in the posterior parietal cortex encode patterns of bimanual coordination. *Cereb Cortex* 28: 1549–1567, 2018. doi:10.1093/cercor/bhx052.
129. **Mooshagian E**, **Holmes CD**, **Snyder LH.** Local field potentials in the parietal reach region reveal mechanisms of bimanual coordination. *Nat Commun* 12: 2514, 2021. doi:10.1038/s41467-021-22701-3.